UiT The Arctic University of Norway

Faculty of Biosciences, Fisheries and Economics, Department of Arctic and Marine Biology

The structure of nasal conchae in Svalbard rock ptarmigan (*Lagopus muta hyperborea*) with comparisons to three other Galliform birds

Marie Aas Westvik

BIO-3950 Master's thesis in Biology, May 2022

Cover photo by M. Westvik: Two female Svalbard rock ptarmigan on Sarkofagen, Longyearbyen Sept 4th, 2016.

Foreword

Firstly, I would like to thank my supervisors, L. Folkow and A. Nord, for their excellent supervision and input during the work of this thesis. Your encouragement during a difficult time post-covid infection kept my motivation up and going.

I have outsourced a bit of work as a part of this thesis. Hence, a big thanks to the PETcore team represented by M. Martin-Armas for the enthusiasm and joy of scanning chopped-off bird heads. Second, I would like to thank the Department of Clinical Pathology at UNN, represented by T. Mortensen, for splendid work with the histological slides. They've received many compliments from all that have laid eyes on them. Last, but not least, thank you to the Advanced Microscopy Core Facility at UiT represented by R. Mortensen for making excellent digital images of these slides.

Lab technicians at AAB and AMB provided guidance and help when needed in the lab. I thank you for a safe and healthy time in the labs. Also, my fellow classmates have provided joy and laughter every day at our office. I thank you for two great years together.

I would also like to thank my nurse colleagues at UNN for showing interest in my thesis, even though I've had my fair share of odd and questioning looks. Finally, a collective thanks to my family and friends that have showed interest in my work during the past 10 months.

I am (finally) done with in total 8 years of studies in 7 years here at UiT (including a couple of exchanges), and I am now ready for new and exciting adventures. I thank you for 7 great years at the most spectacular campus in Norway, maybe I'll even return some day.

Tromsø, May 2022

Marie Aas Westvik

Abstract

Birds are endothermic homeotherms that regulate internal metabolic heat production to keep a stable body core temperature. Lung ventilation, which is required to obtain oxygen for metabolism, is potentially a large source for heat and water loss. In a polar habitat with low year-round temperatures and scarcity of food in the winter, conservation of heat and water is crucial for survival of the resident Galliform bird Svalbard rock ptarmigan (*Lagopus muta hyperborea*). Nasal conchae are important for minimizing respiratory heat and water losses, a process known as nasal temporal countercurrent heat exchange (NHE). These are cartilaginous scroll-shaped and mucosa-lined structures protruding into the nasal cavity of birds. Heat and water conservation is assumed to be more important in species adapted to very cold or dry habitats, as conservation of the limiting resource is crucial for species survival in such habitats. More elaborate conchae would therefore be beneficial. Hence, I hypothesized that Svalbard rock ptarmigan, adapted to a polar habitat, have more elaborate nasal conchae than the domestic chicken (*Gallus gallus domesticus*), adapted to a temperate habitat, with mainland rock ptarmigan (*Lagopus muta*) and willow ptarmigan (*Lagopus lagopus*) being intermediate. To investigate this, head specimens of all study birds were obtained. Computed tomography (CT) scans of the heads were made, including histologic investigations of the nasal conchae in Svalbard rock ptarmigan. Finally, the potential importance of NHE in reducing respiratory heat loss in the Svalbard rock ptarmigan was estimated and compared to existing metabolic data. CT scans revealed that Svalbard rock and willow ptarmigan had larger conchal surface areas than the domestic chicken, the Svalbard rock ptarmigan having the largest conchal surface area of all study birds independent of body size differences. Scaled to volume of air space, the willow ptarmigan exceeded the Svalbard rock ptarmigan. 62.7 % of the heat added upon inhalation could be conserved during exhalation, assuming that NHE may help reduce the exhaled air temperature of the Svalbard rock ptarmigan from 40 °C to 20 °C in a -10 °C environment. This corresponds to a 18.0 % reduction in metabolic costs of the total resting metabolic rate. In conclusion, I present evidence that may point to conchal adaptation to habitat in the domestic chicken, the Svalbard rock ptarmigan and the willow ptarmigan, also exemplifying how NHE may contribute substantially to heat conservation.

Key words: Svalbard rock ptarmigan, chicken, Galliformes, nasal conchae, turbinate, thermoregulation, nasal heat exchange, CT scan, histology

List of abbreviations

AVA: arteriovenous anastomose

BCE: before common/current era

Mucus glands: multicellular intraepithelial glands

NHE: nasal temporal countercurrent heat exchange, i.e., nasal heat exchange

pt: ptarmigan

RMR: resting metabolic rate

SA: surface area

SD: standard deviation

T_a: ambient air temperature

T_b: body core temperature

T_e: exhaled air temperature

Anatomical plane specific terms

Rostral/rostrally: towards the head

Caudal/caudally: towards the tail(bone)

Median: in the centre

Lateral/laterally: away from the centre

Dorsal/dorsally: towards the back

Ventral/ventrally: towards the belly

Table of Contents

1 Introduction

The great diversity of animals that we see today is a result of evolution over millions of years, according to Darwin's theory of evolution. Closely related species can differ in morphological traits; one of the best-known examples being beak size and shape in the Galápagos finches (order Passeriformes, family Thraupidae) (Sulloway, 1982). Specific feeding habits were hypothesized to be the main cause for this divergence. Also other factors, such as geographical distribution or climate, can cause natural selection for better adaptation to the respective habitat (Darwin, 1882). The outcome of evolution is often most easily seen on external macroscopic structures, like the beak of birds. As another example, birds living in colder habitats have smaller beaks than birds living in warmer habitats, heat conservation in the colder habitats being the main driver behind this adaptation to habitat (e.g., Danner & Greenberg, 2015). There is, however, great variation in internal nasal structures among birds (Bang, 1971), but what exact factors that cause this variation still remain somewhat unclear. Thus, questions arise to whether these differences are caused by environmental factors like climate, and why they could be important as birds inhabit a wide range of different habitats.

1.1 Thermoregulation and respiration

Birds and mammals are endothermic homeotherms. That means they use internal metabolic heat production to maintain a favourable body core temperature (T_b) within a narrow range (Angilletta et al., 2010), largely independent of ambient air temperature (T_a) (Irving & Krog, 1954; Prinzinger et al., 1991; Scholander et al., 1950). The maintenance of a rather stable T_b is done by thermoregulation, that being physiological or behavioural processes like changes in pelage/plumage conductance, circulation, posture or metabolism as a final resort (Angilletta et al., 2010). Oxygen needed for metabolic heat production is provided by respiration, and the inhaled air must be saturated with water vapour and heated to T_b prior to its entry into the lungs (Cole, 1954). This is to protect the sensitive lung tissue from being damaged (Walker et al., 1961), and to facilitate gas exchange in the alveoli (Negus, 1958). However, Walker et al. (1961) estimated that up to 75 % of the heat and water added upon inhalation is lost during exhalation in human respiration. Thus, humans do not possess efficient heat conservation mechanisms, and what is lost must continuously be replaced by metabolic heat production. Hence, respiratory heat and water losses could potentially be challenging for many free-living birds and mammals, as access to food and water can be restricted for parts of the year. Contrary to humans, wild animals are often more efficient in conserving heat and water lost in

respiration. For example, the polar Adélie penguin (*Pygoscelis adeliae*) recovers 81.9 % of the water and 83.4 % of the heat from its exhaled air (Murrish, 1973). The winter-acclimated Eurasian reindeer (*Rangifer tarandus*) can recover 65 % of the heat added to inhaled air upon exhalation (Blix & Johnsen, 1983). Nasal breathing is by far the primary way of breathing in birds and mammals, as opposed to oral breathing (Owerkowicz et al., 2014). Thus, selection for nasal structures that conserve heat and water has been important for adaptation to habitat.

1.2 Nasal air flow and nasal heat exchange in birds

Avian nasal conchae (mammals: turbinates) are bilaterally paired, cartilaginous scroll-shaped and mucosa-lined structures protruding into the nasal passages from the lateral nasal cavity walls (Bang, 1971; Schmidt-Nielsen et al., 1970). They can be distinguished as three different entities: rostral (anterior), middle (maxillary/respiratory) and caudal (olfactory/posterior) conchae (Bang, 1971; Danner et al., 2017). Certain birds in the order Galliformes (fowl and allies), like the domestic chicken (*Gallus gallus domesticus*) and the wild turkey (*Meleagris gallopavo*), have a 4th pair of conchae, atrial conchae (Bang, 1971; Bourke & Witmer, 2016). Most of the heat and water exchange take place in the middle conchae, while the caudal conchae are the main site of olfaction (Bang & Wenzel, 1985; Negus, 1958). The air flow through the nasal cavity with its conchae is presented schematically in Figure 1. The atrial and rostral conchae in particular direct air to specific regions of the nasal cavity (*cavum nasi*), thereby working as baffles. For example, the rostral conchae produce a channel of air directed towards the caudal conchae, thereby facilitating olfaction (Bourke & Witmer, 2016). Also, they direct the air around the end of the rostral conchae (*crista nasalis*), where fluid secretions from nasal glands are temporarily stored in a concave-like reservoir. Dry air moving over this reservoir of fluids picks up some moisture before entering the middle conchae, where the main heat and water exchange take place (Bang & Wenzel, 1985; Bourke & Witmer, 2016).

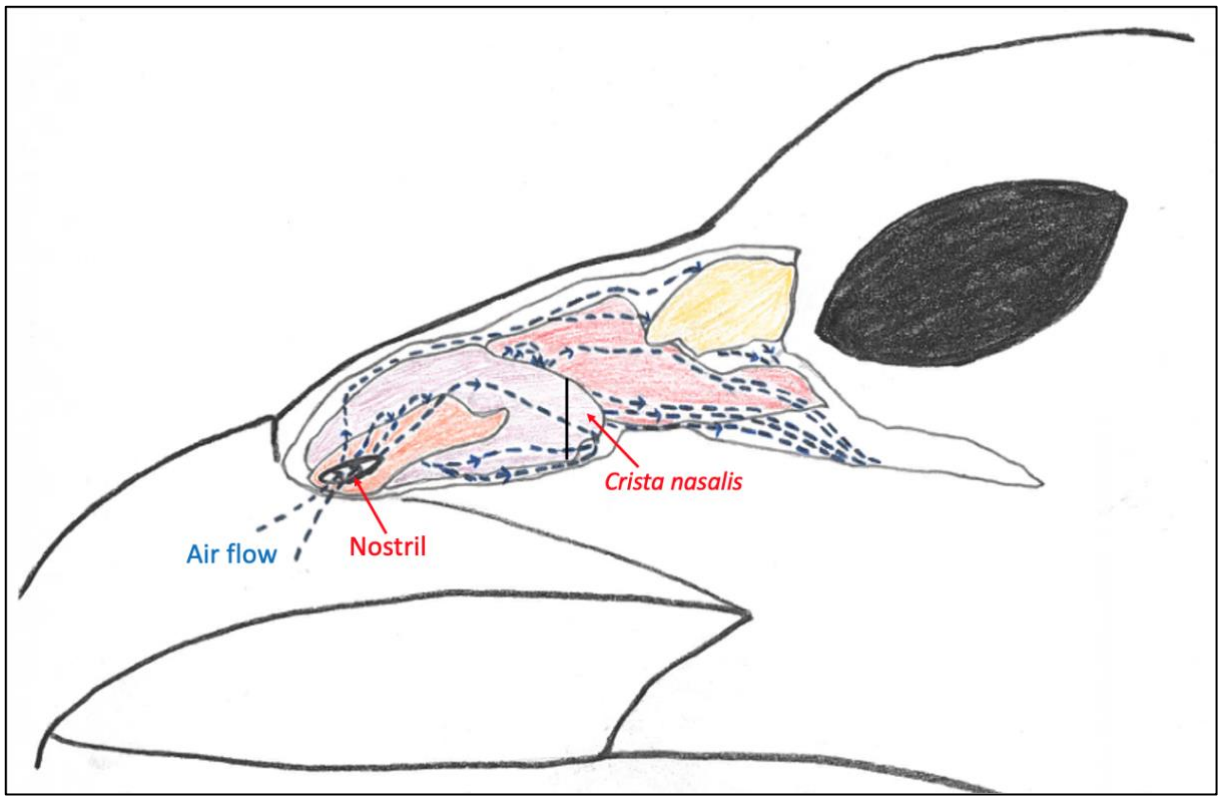

*Figure 1: The air flow in a turkey nose. Air (dashed blue lines) enters the nostril, moves around the atrial concha (orange), along the nasal cavity wall and on all sides of the rostral concha (purple). It rounds the end of the rostral concha (*crista nasalis*), moving along the middle concha (red) on all sides. Air flowing along the top cavity wall descends behind the caudal concha (yellow) and exits the nasal cavity through an opening to the oral cavity (*cavum oris*, not shown). Obviously, air also flows inside the atrial, rostral, and middle conchae. No scale. Drawing by M. Westvik, inspired after figure from Bourke and Witmer (2016).*

The regulation of heat and water content in the air is controlled by a countercurrent heat exchange mechanism in the nasal mucosa (nasal temporal countercurrent heat exchange; NHE), as seen in Figure 2a: Cold inhaled air is warmed and saturated with water vapour by the well-vascularized mucosal surface lining the inside of the nasal cavity. This leaves the mucosal surface cooled down, with surface temperatures being the lowest closest to the nostrils and increasing progressively towards the caudal end; i.e., a temperature gradient is established (Jackson & Schmidt-Nielsen, 1964). It has been hypothesized that the well-vascularized mucosa can remain colder than T_b because blood may be routed in a countercurrent fashion. This is based on anatomical and model studies of reindeer (Johnsen et al., 1985). During exhalation, warm and saturated air flowing over the now colder mucosal surface will give up both heat and water back to the mucosal surface. Air leaving the nasal passages is thereby subsequently colder and less saturated in water so that both heat and water losses are kept low (Jackson & Schmidt-Nielsen, 1964).

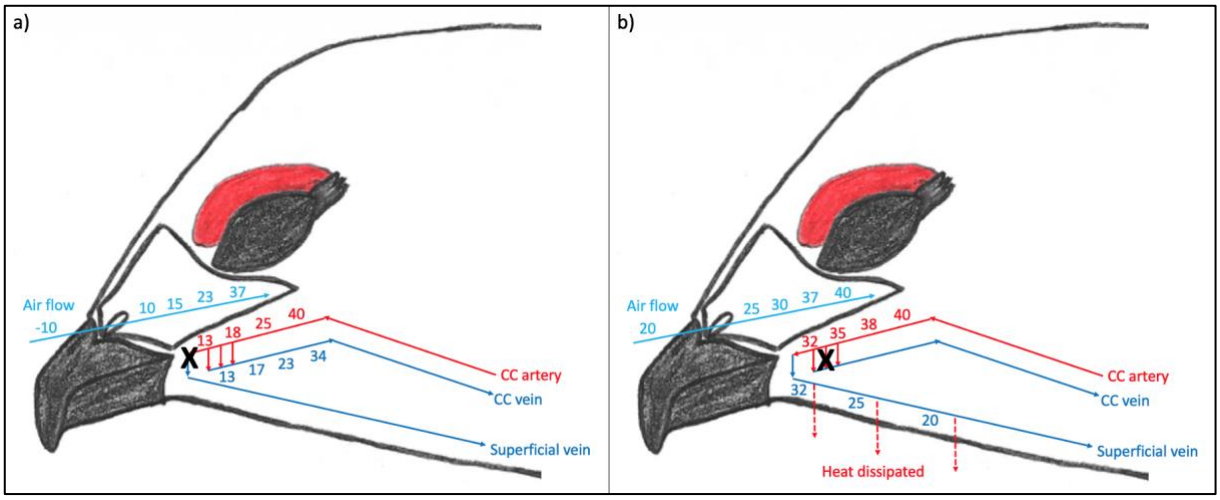

Figure 2: a) An illustration of how the NHE may work during inhalation in a Svalbard rock ptarmigan nose, with hypothetical values and placement of blood vessels. Heat is transferred from the warm arterial blood in a countercurrent (CC) artery, thereby heating the air and leaving the blood colder. This gradient is maintained by countercurrent (CC) veins that runs near the CC artery. Heat is, in this way, short-circuited. Drainage by superficial veins is shut off (X), for example by constriction of arteriovenous anastomoses (AVAs: shunts between arteries and veins that allows blood to bypass capillary networks (Midtgård, 1989a)). b) When the NHE is not used (X), for example during heat stress. Blood is now drained by superficial veins, and heat is lost rather than conserved. Drawing by M. Westvik.

Murrish and Schmidt-Nielsen (1970) list four main factors that affect the effectiveness of the NHE: 1) the surface area available for heat and water exchange, 2) the distance from the centre of the air flow to the nearest surface, 3) the velocity of the air flow over this surface and 4) the blood flow in the nasal mucosa. In other words, a large surface area (i.e., elaborate conchae), a low air flow velocity and a short distance from the centre of the air flow to the mucosal surface would all facilitate heat and water exchange. The last factor, the blood flow, is subjected to physiological control. Countercurrent blood flow is favoured in situations where heat and water conservation is crucial (Figure 2a), while unidirectional flow and drainage by superficial veins happens in a state of heat excess (Figure 2b) (Johnsen et al., 1985). Adrenergic vasomotor responses cause these adjustments, such as constriction of AVAs by adrenalin/noradrenalin (Folkow, 1992; Murrish, 1973). For example, exhaled air temperature (T_e) has been found to decrease with a decreasing T_a in both summer- and winter-acclimated reindeer (Blix & Johnsen, 1983). However, T_e in summer-acclimated reindeer was much lower than in winter-acclimated reindeer, at one and the same T_a. Hence, Blix and Johnsen concluded that the effectiveness of NHE is regulated according to the total thermal situation, as winter-acclimated reindeer have pelage of better insulative value than summer-acclimated ones. The same situation is described for Adélie penguins (Murrish, 1973).

1.3 Adaptation to habitat

Mammalian turbinates have been more studied than avian conchae (e.g., Folkow et al., 1988; Huntley et al., 1984; Johnsen et al., 1985; Van Valkenburgh et al., 2011). Few studies have investigated for turbinate adaptation to habitat. One example is Mason et al. (2020), where they found larger and more elaborate turbinates in high-latitudinal polar seals compared to their lower-latitudinal tropical relatives. Furthermore, Van Valkenburgh et al. (2011) did show that total turbinate and respiratory surface area correlated well with body mass, larger carnivores having smaller turbinates. Also, the ratio of olfactory to respiratory surface area was 1:3 in aquatic carnivores, while the inverse was true for terrestrial carnivores. Van Valkenburgh et al. (2011) concluded that olfaction is important for terrestrial carnivores in locating prey, while other factors have selected for less olfactory and more respiratory surface area in aquatic carnivores. Enhanced need for heat and water conservation could be a potential factor. Hence, turbinal size is therefore, to some extent, fixed due to evolutionary adaptation to climate in the respective habitat. However, Midtgård (1989a) found that cold-exposed chickens (i.e., cold-acclimated chickens) developed more AVAs in the eyelids, wattle, and comb than chickens in a control group. AVAs allow a finer control of blood flow from the body core to peripheral parts, thereby being important in thermoregulation and cold protection of peripheral tissues. In addition, the density of AVAs was higher in the mucosa of the rostral conchae in heat-exposed chickens compared to controls (Midtgård, 1989b). Hence, acclimatization to present conditions, for example temperature, can impact the development of microanatomical structures important in thermoregulation.

1.3.1 Selected study birds and their respective habitats

To the best of my knowledge, there are no comparative studies investigating conchal adaptation in birds on a latitudinal gradient, where climate in the respective habitat (e.g., polar, temperate, tropical etc., after the Köppen-Geiger climate classifications (Beck et al., 2018)) is the main factor for possible adaptation. The Svalbard rock ptarmigan (*Lagopus muta hyperboea*) is a subspecies of the rock ptarmigan (*Lagopus muta*). It is endemic to Svalbard, an archipelago situated in the high-Arctic (74-81° N) (Løvenskiold, 1954). This high latitudinal location results in great seasonal variations in light conditions with rather low temperatures year-round. From complete darkness in winter to 24 hr sunlight in summer, resident animals, like the Svalbard rock ptarmigan, must adapt to these extreme changes (Norderhaug, 1984). The Svalbard rock ptarmigan therefore has a striking change in annual body weight, being about 600 g by the start of spring and fattening up about 1100 g by the

end of autumn (Mortensen et al., 1983). This increased amount of fat works as both an energy storage when food is scarce in the winter (Mortensen et al., 1983) and to some degree as insulation (Mortensen & Blix, 1986). They also decrease the energetic cost of locomotion in winter, despite the increase in body weight (Lees et al., 2010; Lindgård et al., 1995). The Svalbard rock ptarmigan is clearly adapted to life in a polar habitat, but their nasal conchae has not yet been studied. It would therefore be interesting to investigate if their conchae also are adapted to a polar habitat, as heat and water conservation would be important in such a hostile habitat.

For comparisons, there are two species of ptarmigan living in mainland Norway, rock ptarmigan and willow ptarmigan (*Lagopus lagopus*). The climate in the northern parts of Norway is intricate, being warm-temperate along the coast to cold-temperate and possibly even polar further inland (Beck et al., 2018). The transitions are fluid. Hence, the conchae of these ptarmigan might differ from those of the Svalbard rock ptarmigan if selection for better adaptation to habitat is the case. The rock ptarmigan has a circumpolar distribution, found in barren and higher grounds. It also occurs in mountainous areas such as the Alps and the Pyrenees (Løvenskiold, 1964). It has a fairly constant weight year-round, the average being 487 ± 36 g in northern Norway (Mortensen et al., 1985). The willow ptarmigan has a similar circumpolar distribution as the rock ptarmigan. However, it is also found in lower and more forested grounds (Pedersen et al., 2021). It has a relatively constant body weight year-round of 598 ± 62 g on average in northern Norway (Mortensen & Blix, 1986). Rock, Svalbard rock and willow ptarmigan all have seasonal changes of plumage as a response to changing light conditions, being white in the winter and grey/brownish in the summer (Høst, 1942). Air-filled barbules of their feathers are improving the insulative value of their plumage (Dyck, 1979). Reducing the resting metabolic rate (RMR) as a part of winter acclimation is also a way in which these birds save energy during the harsh winters (Mortensen & Blix, 1986).

All three ptarmigan are galliform birds, like the domestic chicken. The domestic chicken is believed to originate from the wild red junglefowl (*Gallus gallus*) populations in China, originally adapted to a (sub)-tropical habitat. As poultry husbandry was integrated in the Shang Dynasty around 1600 BCE, the domesticated chickens could now adapt and survive in more temperate areas, partly due to sheltering and constant feeding. Today, the chicken is found across all continents and is the most numerous of the domesticated animals. This, and intensive breeding, has resulted in a great variation of weight, appearance, and behaviour among the many different breeds that exists today (Peters et al., 2016). The need for heat and

water conservation might therefore not be as crucial for the chicken. Hence, including the chicken in this thesis could therefore enlighten possible evolutionary adaptations to habitat in nasal conchae structure among these four galliform birds.

1.4 Main aim and hypothesis

The main aim of this thesis is therefore to study and describe the structure of nasal conchae in Svalbard rock ptarmigan, and investigate for possible variation amongst domestic chicken, rock ptarmigan and willow ptarmigan. I therefore hypothesize that the Svalbard rock ptarmigan, adapted to a polar habitat, possess more elaborate conchae than the domestic chicken, adapted to a temperate habitat, with the rock and willow ptarmigan being intermediate. This will be investigated by analysing computed tomography (CT) images of head specimens of all four study birds. In CT scans x-rays are projected towards an object from different angles. The different density of tissues produce contrasted image sequences that can be digitally analysed (Brekke et al., 2018). These scans will be complemented with histological analyses of the Svalbard rock ptarmigan conchae, to identify structures/tissues of importance for heat and water exchange. Finally, the potential importance of NHE will be addressed by estimating respiratory heat loss in a hypothetical Svalbard rock ptarmigan. The results will be compared to existing metabolic data (e.g., Mortensen & Blix, 1986; Nord & Folkow, 2018).

2 Methods

2.1 Terminology

Concha nasalis is the scientific Latin name given for these internal nasal structures in both mammals (NAV, 2017) and birds (Baumel et al., 1993). There is, however, an interchangeable use of the terms conchae and turbinates in the literature, especially when addressing these structures in birds (e.g., Hillenius, 1992). Generally speaking, turbinates are used to describe the bony mammalian nasal structures (Negus, 1958; Owerkowicz et al., 2014), while the cartilaginous avian nasal structures are referred to as conchae (Bang, 1971; Owerkowicz et al., 2014). Therefore, the term 'conchae' is used when addressing these nasal structures in birds in this thesis.

2.2 Sampled material

Wild birds of Svalbard rock ptarmigan are captured near Longyearbyen (78°13'N 15°33'E) on a regular basis and kept at the approved animal research facility 'Avdeling for Arktisk Biologi' (AAB) at UiT The Arctic University of Norway, campus Tromsø. Chicks were hatched from eggs laid by captive females in 2015 and 2017. They were subjected to a natural Tromsø photoperiod either outdoors or artificially indoors. Seven of these adult birds were originally used for other scientific purposes (Permit no. 14209, approved 31st Oct 2018 by the Norwegian Food Safety Authority), but when decapitated on 18th Dec 2020 the heads were immediately fixed in 4 % paraformaldehyde (PFA). They were transferred to 0.4 % PFA in Feb 2021. Frozen specimens (i.e., heads) of rock ptarmigan, Svalbard rock ptarmigan and willow ptarmigan were also used, the rock and willow ptarmigan of a wild origin (Indre Troms, appr. 68°50'N 19°34'E). A 14-week-old domestic chicken (mixed breeds, 25 % Sussex) was euthanized according to approved methods by its private owner. It was decapitated post-mortem and the head was donated to this study. It was immediately freeze-stored at AAB in <-20 °C until further analysis. See Table 1 for an overview of the specimens that were used in this thesis.

*Table 1: An overview of the different specimens that were available. The state of the specimens and in what analysis they were used are given, along with age, body mass, sex, and origin when known. Body masses (mean ± SD) from literature are included as original body mass was unknown for most specimens. These are marked with an *. pt = ptarmigan*

Bird	State	Analysis	Age	Body mass	Sex	Origin
Chicken	Frozen	CT scan	14 weeks	*948 g	Male	Captive, local
Rock pt	Frozen	CT scan	-	*456 ± 16 g	-	Wild, Indre Troms
Svalbard pt	Frozen	CT scan	-	*705 ± 56 g	-	Captive, AAB
Svalbard pt	Frozen	Dissection	6 yrs	1036 g	Male	Captive, AAB
Svalbard pt	Fixed	Histology	3 or 5 yrs	**767 ± 69 g	-	Captive, AAB
Willow pt	Frozen	CT scan	-	*658 ± 59 g	-	Wild, Indre Troms

*Body masses from literature. Body masses included are from Batkowska et al. (2015) for chicken (in this case 12 weeks old), and Mortensen and Blix (1986) for winter-acclimated birds of rock, Svalbard rock and willow ptarmigan.

**Mean body mass of the seven birds in Sept 2020. Four of them were fixed, but the IDs of which ones were unknown.

2.3 Dissection

The head of a frozen Svalbard rock ptarmigan was skinned. A longitudinally cut with a hacksaw blade was made in the sagittal plane, dividing the head in a left and right part (Figure 3a). The cut was made distal to the median plane so that the whole left nasal passage remained untouched (Figure 4).

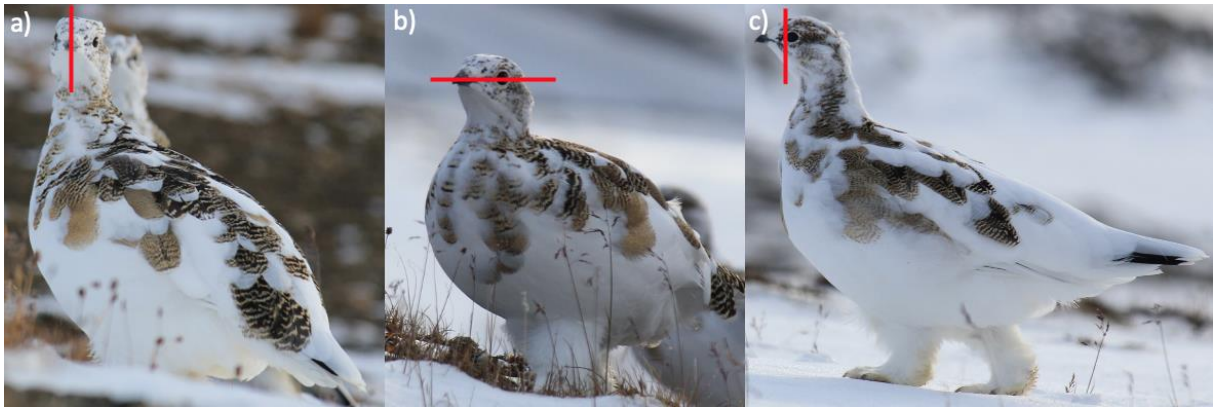

Figure 3: The different planes of the Svalbard rock ptarmigan body: a) sagittal plane (median plane is used when the body is divided in two symmetrical left and right parts), b) horizontal plane, and c) frontal plane. These planes are also known by other nomenclature, but these are the terms used in this thesis.

Placed under a Wild Heerbrugg M3B Stereo Microscope (Wild Heerbrugg AG, Heerbrugg, Switzerland), tissue was removed part by part to reveal the nasal septum (*septum nasi*; Figure 4b). The nasal septum divided the nasal cavity in two separate and bilaterally symmetrical parts, each associated with one nostril (*naris*). The septum was then removed, and the conchae (*conchae nasalis*) identified (Figure 4c). All conchae were attached to the lateral wall of each nasal passage, with the rostral conchae surrounding the nostril openings.

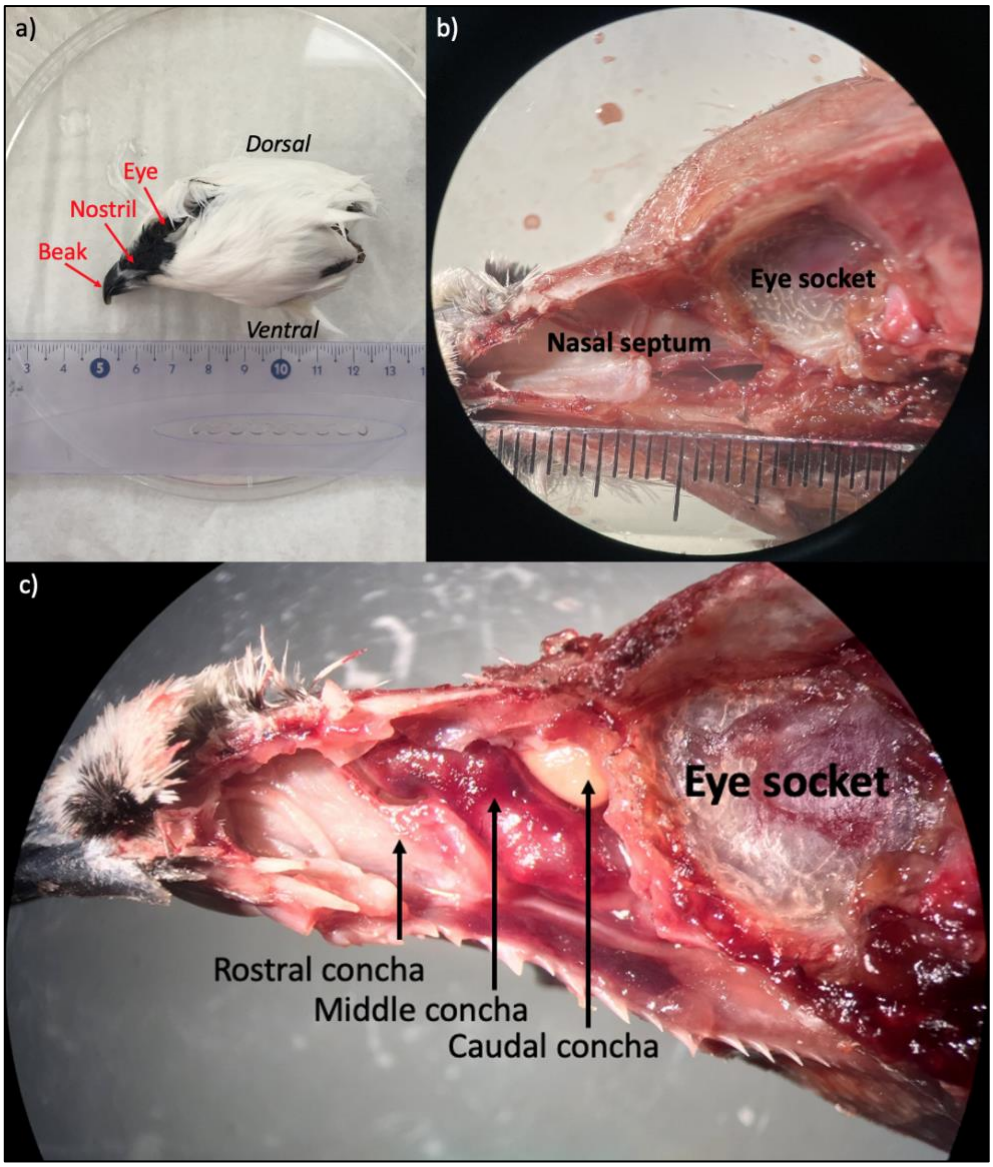

*Figure 4: a) A fixed Svalbard rock ptarmigan head with naming of key parts and anatomical plane specific terms. Notice that the whole head apart from the beak and the eyes is covered by feathers, including the nostrils. Photo by M. Westvik. b) A sagittal cut through the right nasal passage of a Svalbard rock ptarmigan, image mirrored. The eye socket (*orbita*) and nasal septum are marked, the beak pointing to the left in the image. Taken through a stereo microscope by L. Folkow. Scale bars in millimeters. c) The nasal septum removed revealing the conchae, image mirrored. The eye socket and three main conchae are marked, the beak pointing to the left in the image. Same specimen as in b), without scale bar. The lower part of the beak has been removed. Taken through a stereo microscope by M. Westvik.*

2.4 CT scanning

Histology of fixed bird specimens has been the traditional way to study avian conchal structures, as their cartilaginous nature is not well-preserved in the making of dry museum study skeletons (Danner et al., 2017). However, recent year's technological development has opened new, more efficient, and non-invasive ways of obtaining both physiological and anatomical knowledge, for example by CT scans. Therefore, frozen head specimens of all study birds (n=4 in total) were thawed and prepared for CT scans by flushing air through the nostrils to clear them for any fluid content, before sealing them in leakage-proof vacuum bags (they were *not* vacuum packed, *only* sealed with the heating function of a vacuum sealer). The CT scans were performed at the Preclinical PET Core Facility, located in the PET Imaging Center of the University Hospital of North Norway (UNN). Samples were scanned with an X-RAD SmART (Precision X-Ray, Madison, CT USA) at 80.00 kV, 1.500 μA and a slice thickness of 100 μm. The image sequences were in DICOM (.dcm) file format.

2.4.1 Image processing and analyses

The free and open-source code software Horos™ (version 3.3.6, Horos Project, Nimble Co., Annapolis, MD USA) was used to take five repeated measurements of nasal cavity depth, length and width respectively. Basic adjustment of brightness was done to identify relevant structures, in accordance with (the rather sparse) general guidelines for scientific image processing (Cromey, 2010; Rossner & Yamada, 2004). Microsoft® Excel for Mac (version 16.55, Microsoft Co., Redmond, WA USA) was used to calculate a mean value for each variable respectively.

The main image processing and analysis were done in ImageJ (version 1.53k, Schneider et al., 2012), a free and public software to analyse scientific images. Quantification of the total inner surface area of the nasal cavity, individual conchal surface areas and area of air space for volume estimation were the overall goal of this analysis. However, digital images of the thin conchae can be problematic to analyse, as levels of brightness and/or contrast must be adjusted to separate the conchae from the rest of the image (Figure 5a). Firstly, the number of pixels that 'represents' the conchae are few. In addition, these have low brightness values, i.e., it is difficult to distinguish between conchae and background noise from the scan when brightness or contrast for the whole image is adjusted (Van Valkenburgh et al., 2011).

Hence, contrast limited adaptive histogram equalization (CLAHE) is an image processing technique that increases the contrast in the parts of an image that needs it instead of the whole

image. The low-contrasted conchae will greatly benefit from this, while the already high-contrasted bone will not be much affected (Figure 5a vs. 5b). Hence, over-saturation of some structures in the image is prevented (Van Valkenburgh et al., 2011). The ImageJ plugin CLAHE (Saalfeld et al., 2022) was applied to image sequences in the frontal plane of all study birds (default settings of block size 127, histogram bins 256 and maximum slope 3.00; see Appendix 1 for further explanations). The ImageJ measuring tool was used to measure the inside perimeter and area every 0.5 mm (every 5th image) along the nasal cavity and its conchae (Figure 5c). Each concha was also measured separately, including the nostril openings. All measurements were repeated three times to calculate mean values. These were plotted and structured in Microsoft® Excel before final analysis in RStudio (R version 4.0.3, R Core Team, 2020; RStudio version 1.3.1093, RStudio Team, 2020) with the gg2plot package (Wickham, 2016). Middle concha scrolling was determined by measuring their extended lengths five repetitive times at the place of maximum scrolling (determined by eyesight) and calculate mean values. Since detailed data on body mass were lacking, the assumed size differences between the study birds (Table 1) were considered by scaling conchal surface areas to volume of air space of their nasal cavities. Volume of air space is probably the variable that limits, and relates most closely, to conchal surface area and shape (Van Valkenburgh et al., 2011).

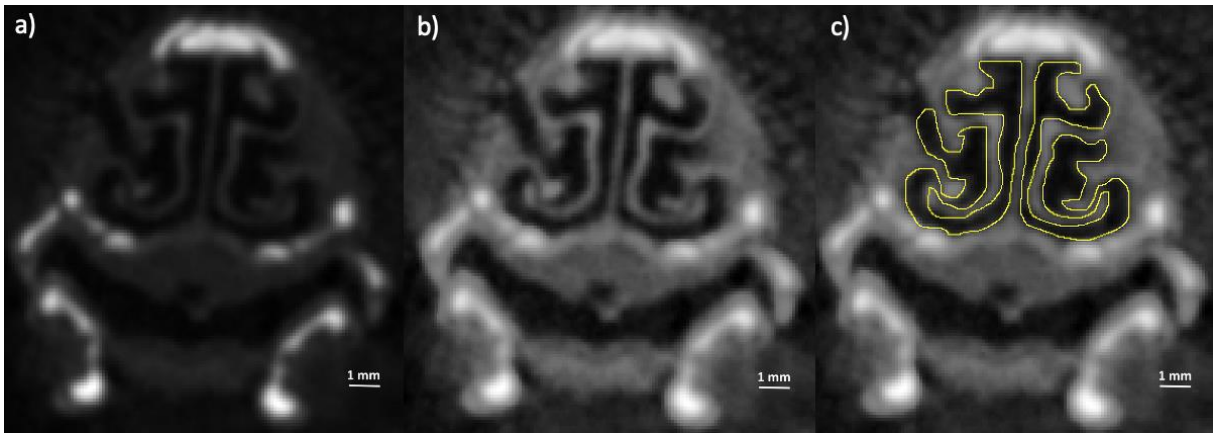

Figure 5: Image processing on a CT image of the nasal cavity of a Svalbard rock ptarmigan in the frontal plane. There is a greyscale spectrum from black to white, where black is air (least dense) and white is bone (most dense). Other tissues are in different shades of grey depending on their density. a) The original CT image, b) the same image processed with CLAHE (the grey areas outside the bird head are noise made visible) and c) how the measuring tool in ImageJ was used to estimate the perimeter and air space area every 0.5 mm. Oriented dorsal (top) to ventral (bottom).

2.5 Histology

An overview of the gross (or macro-) anatomy of the conchal structures were achieved by dissections and CT scans. To study the microanatomy, however, histology and the making of

histological slides for microscopy is a traditional and well-based method (e.g., Hussein et al., 2015). A 4/0.4 % PFA fixed Svalbard rock ptarmigan head was skinned and rinsed in running tap water. 83 g of EDTA was dissolved in 583 mL of distilled water and adjusted to pH 8 by addition of approximately 9 g NaOH. This gave an approximate ratio of 1:20 tissue : solution, as recommended for decalcification of bone tissue to allow sectioning (Gamble & Bancroft, 2008; Kiernan, 2008). The beaker with solution and head was left on an AREX Digital (VELP® Scientifica Srl, Italy) hot plate stirrer at 50 rpm (room temperature; no heating) for 3 weeks with weekly change of EDTA solution. Endpoint testing was conducted with the ammonium oxalate test for every change of solution, slightly adjusted from Rosen (1981): 5 mL of used EDTA solution was transferred to a test tube before addition of 5 mL of saturated ammonium oxalate ($(NH_4)_2C_2O_4$) solution. It was left to stand for 30 minutes. Oxalate ($C_2O_4^{2-}$) precipitates free calcium ions (Ca^{2+}), so if these are present in the solution a white precipitate forms and the decalcification process is not finished. A clear solution after 30 minutes indicates that the sample is decalcified as there is no or few calcium ions left in the solution, i.e., there are no more calcium left in the bone.

The head was subsequently rinsed in running tap water, cut in two sections of 4-5 mm thickness in the frontal plane (Figure 6b), and placed in tissue cassettes in 0.4 % PFA. These were delivered to the Department of Clinical Pathology at UNN, where dehydration, clearing, infiltration, embedding and staining (haematoxylin and eosin staining; H&E) were done.

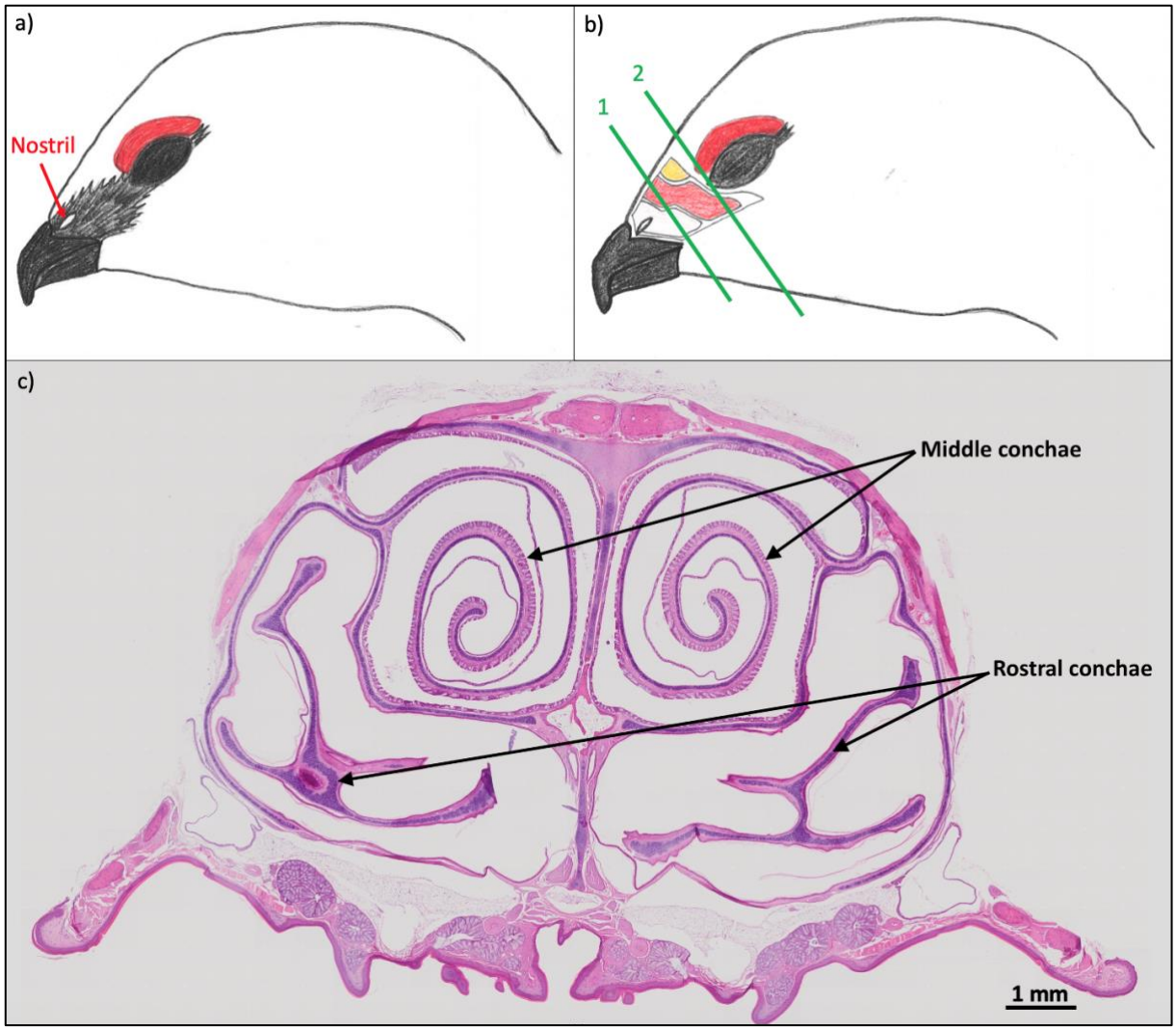

*Figure 6: a) An illustration of a Svalbard rock ptarmigan head in profile with nostril marked. b) The same illustration with the nasal cavity and its conchae added; rostral concha in white, middle concha in red and caudal concha in yellow. No scale. Illustrations by M. Westvik. The green lines mark the approximate locations of the histological sections. c) An example of the resulting histological slides from section 1. The rostral and middle conchae are marked with black arrows. Oriented dorsal (top) to ventral (bottom), the ventral edge being the palate (*palatum*).*

The resulting histological slides (one example in Figure 6c) were scanned with an Olympus VS120 Virtual Slide Microscope (Evident Corporation, Tokyo, Japan) at 20x magnification to make digital images. The images were analysed in OlyVIA (version 1.0.6c37, Evident Corporation, Tokyo, Japan) with the aid of colour and text atlases of histology and cytology (Kuehnel, 2003; Young et al., 2006). The thickness of the different tissues was estimated with the scale bar tool in OlyVIA. Existing literature on nasal histology in chicken (Watanabe et al., 2020), geese (Harem et al., 2018), and birds in general (Bang, 1971) were used in the discussion of these results.

2.6 Respiratory heat loss

Energy conservation is, as stated in the introduction, important for winter survival in the polar Svalbard rock ptarmigan. Therefore, the daily respiratory heat loss rates of a hypothetical 1 kg Svalbard rock ptarmigan with T_b = 40 °C resting in T_a = -10 °C were estimated, to address the efficiency of NHE. It was assumed that in a state of countercurrent blood flow in the nasal mucosa, T_e = 20 °C (i.e., NHE is conserving heat and water), while in a state of unidirectional blood flow T_e = 40 °C (i.e., NHE is not conserving any heat or water). The halved hypothetical reduction in T_e between these two states were based on findings from Geist (2000) and Schmidt-Nielsen et al. (1970) on the efficiency of NHE in other avian species.

The expected minute volume respiration (V_{min}) of a 1-kg bird was calculated based on an allometric equation for birds (r^2 = 0.94), originally developed by Lasiewski and Calder (1971) and improved by Frappell et al. (2001):

$$V_{min}(mL/min) = 386 * Mass^{0.72} \quad (1)$$

Next, water vapour pressures (P_{wx} in the form of P_{w10}, P_{w20} or P_{w40}; units in hPa) at temperatures T_x = -10 °C, 20 °C and 40 °C were calculated with Bolton's equation (Bolton, 1980), using the simplified form from Vömel (2011), and converted to mmHg by 1 Pa = 0.0075 mmHg:

$$P_{wx}(hPa) = 6.112e^{\frac{17.67*t}{t+243.5}} \quad (2)$$

Then the amount of water added to the air upon inhalation (W_a) or lost in exhalation (W_b or W_e; all three represented by W_x, units in mg/min) in V_{min} were calculated with an equation from Blix and Johnsen (1983):

$$W_x(mg/min) = \frac{0.622*P_{wx}}{P_b - P_{wx}} * D_0 * 10^6 * V_{min} \quad (3)$$

Where

W_a: mg/min, water vapour content of air at T_a = -10 °C

W_b: mg/min, water vapour content of air at T_b = 40 °C

W_e: mg/min, water vapour content of air at T_e = 20 °C

D_0: 0.001225 kg/L, density of air at standard temperature and pressure, dry (STPD; 0 °C, 760 mmHg and no water vapour)

P_b: standard air pressure of 760 mmHg

P_{wx}: water vapour pressures at temperatures $T = x$ in mmHg

V_{min}: L/min, respiratory minute volume at STPD

0.662: molar mass of water divided by molar mass of dry air

10^6: number of milligrams in 1 kilogram (mg/kg)

Finally, heat added upon inhalation and heat lost upon exhalation (in J/s; Watts) were calculated with equations from Blix and Johnsen (1983):

$$Heat_{added}(J/s) = \left(\left(\frac{V_{min}}{60\ s/min}\right) * H_c * (T_b - T_a) * D_0\right) + \left(\frac{W_b - W_a}{60\ s/min} * L_h\right) \quad (4)$$

$$Heat_{lost}(J/s) = \left(\left(\frac{V_{min}}{60\ s/min}\right) * H_c * (T_e - T_a) * D_0\right) + \left(\frac{W_e - W_a}{60\ s/min} * L_h\right) \quad (5)$$

Where

H_c: the heat capacity of dry air, 10^3 J/°C/kg

L_h: the latent heat of vaporization, 2.34 J/mg

T_a: ambient air temperature, -10 °C

T_b: body temperature, 40 °C

T_e: exhaled air temperature, 20 °C

60 s/min: the number of seconds per minute

These results were compared to existing RMR data on Svalbard rock ptarmigan from Mortensen and Blix (1986) and Nord and Folkow (2018).

3 Results

The results from the CT scans, image analysis (one specimen of each study bird, n=4 in total) and histology (one specimen of Svalbard rock ptarmigan, n=1) will be used to describe the size and structure of the nasal passages and its conchae in domestic chicken, rock ptarmigan, Svalbard rock ptarmigan and willow ptarmigan. After a general description of their nasal cavities follows a description of each concha, starting rostrally and moving caudally.

3.1 General overview

Table 2 lists the different results from the CT image analyses. According to Figure 7, the domestic chicken had the smallest overlap of rostral and middle conchae, while the Svalbard rock and willow ptarmigan had greater overlaps. The Svalbard rock ptarmigan had the largest absolute conchal surface area (Table 2 and Figure 7d), independent of the assumed body size differences between the study birds (see body masses in Table 1). Excluding the atrial conchae, the caudal conchae were the smallest of all conchae in all study birds (Table 2).

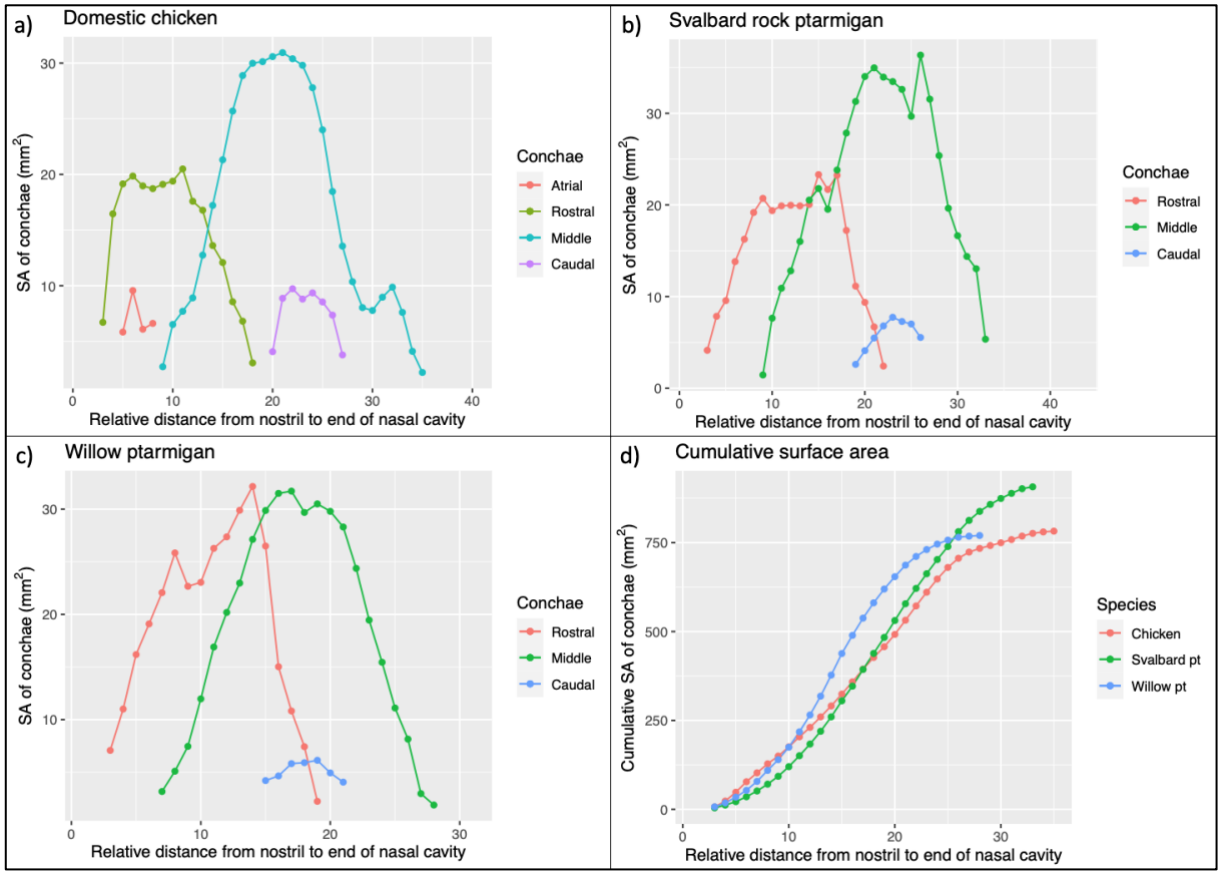

Figure 7: The distribution of surface areas (SA; mm²) from nostril (left) to end of nasal cavity (right). One unit of relative distance on x-axis = 0.5 mm. Individual conchal surface areas in a) domestic chicken, b) Svalbard rock ptarmigan and c) willow ptarmigan. d) Cumulative conchal surface area for domestic chicken (orange), Svalbard rock ptarmigan (green) and willow ptarmigan (blue).

Table 2: Summary of results from the CT image analyses, all in mean ± SD. It was not possible to analyse >50 % of the rock ptarmigan nasal cavity due to collapsed nasal structures and hence lack of air space between the conchae. SA = surface area

Variable	Domestic chicken	Rock ptarmigan	Svalbard rock ptarmigan	Willow ptarmigan
Nasal cavity depth (mm)	10.11 ± 0.20	6.08 ± 0.14	6.77 ± 0.18	8.10 ± 0.17
Nasal cavity length (mm)	21.56 ± 0.09	13.20 ± 0.07	14.45 ± 0.15	15.04 ± 0.06
Nasal cavity width (mm)	10.04 ± 0.13	9.39 ± 0.17	11.16 ± 0.08	10.84 ± 0.12
Total inner nasal SA (mm^2)	2436.41 ± 46.75	-	1815 ± 59.70	1380.08 ± 55.11
Atrial conchal SA (mm^2)	28.11 ± 3.45	-	-	-
Rostral conchal SA (mm^2)	237.36 ± 11.30	-	305.74 ± 13.21	324.67 ± 17.81
Middle conchal SA (mm^2)	456.29 ± 20.61	-	554.61 ± 20.50	409.63 ± 21.24
Caudal conchal SA (mm^2)	60.51 ± 4.70	-	46.53 ± 3.52	35.72 ± 1.70
Total (absolute) conchal SA (mm^2)	782.27 ± 10.02	-	906.88 ± 12.41	770.02 ± 13.58
Volume of air space (mm^3)	1503.85 ± 28.96	-	554.35 ± 16.18	352.70 ± 12.03

Scaled to volume of air space, Svalbard rock and willow ptarmigan had greater surface areas for all conchal measurements compared to the domestic chicken, except for the atrial conchae (Table 3). The ratios were about 1:3 on average for Svalbard rock ptarmigan, while it was about 1:4 on average for willow ptarmigan. The scaled cumulative conchal surface area is shown in Figure 8, the willow ptarmigan having the greatest total conchal surface area as opposed to Figure 7d.

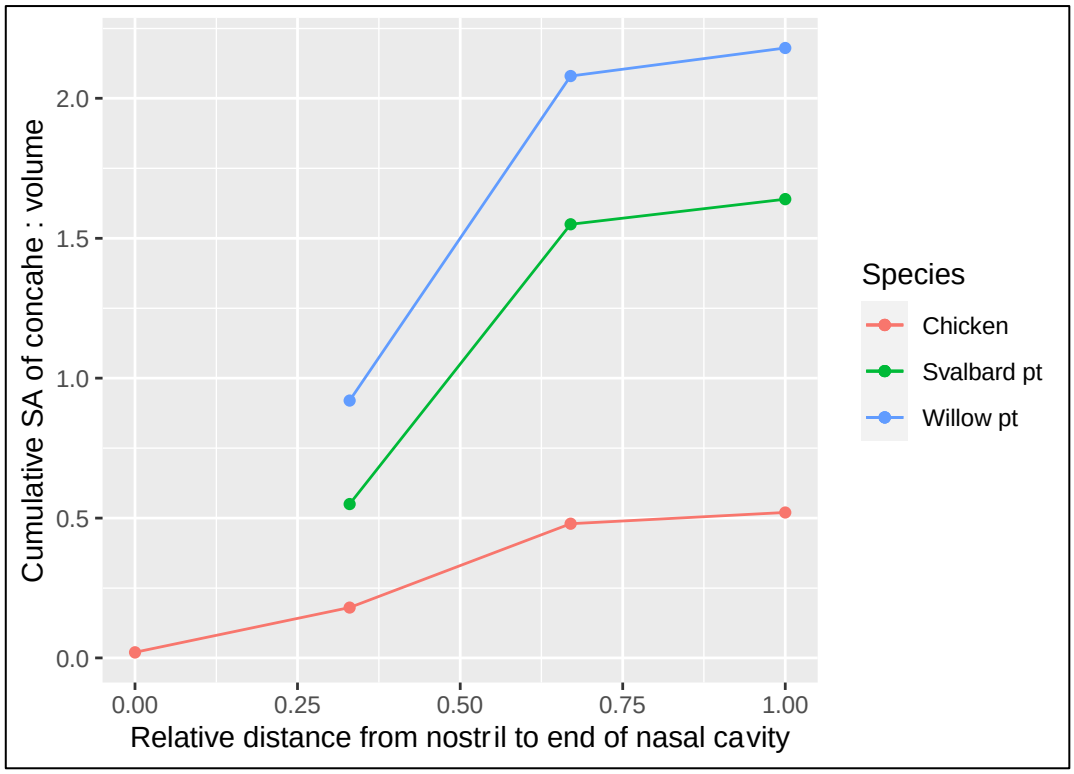

Figure 8: The cumulative conchal surface area (SA) in relation to volume of air space for chicken (orange), Svalbard rock ptarmigan (green) and willow ptarmigan (blue). pt = ptarmigan

Table 3: Relative numbers (ratios) for total inner nasal surface area, individual conchal surface areas and total conchal surface area in relation to volume of air space for each study bird. SA = surface area

Ratios	Domestic chicken	Rock ptarmigan	Svalbard rock ptarmigan	Willow ptarmigan
Total inner nasal SA : volume of air space	1.62	-	3.27	3.91
Atrial conchal SA : volume of air space	0.02	-	-	-
Rostral conchal SA : volume of air space	0.16	-	0.55	0.92
Middle conchal SA : volume of air space	0.30	-	1.00	1.16
Caudal conchal SA : volume of air space	0.04	-	0.08	0.10
Total conchal SA : volume of air space	0.52	-	1.64	2.18

3.2 Atrial and rostral conchae

As mentioned in the introduction, most birds have three main conchae (Figure 4c), but both chicken and turkey have a 4th pair of conchae, the atrial conchae (Figure 1). The atrial conchae were clearly seen in CT images of the domestic chicken in the frontal plane (Figure 9a), in accordance with literature (Figure 9b). They were located laterally to the rostral conchae, facing the nostril openings. Both atrial and rostral conchae were simple curved structures in the domestic chicken, protruding from the ventral and dorsal side of the nasal cavity respectively. The *crista nasalis* was also identified.

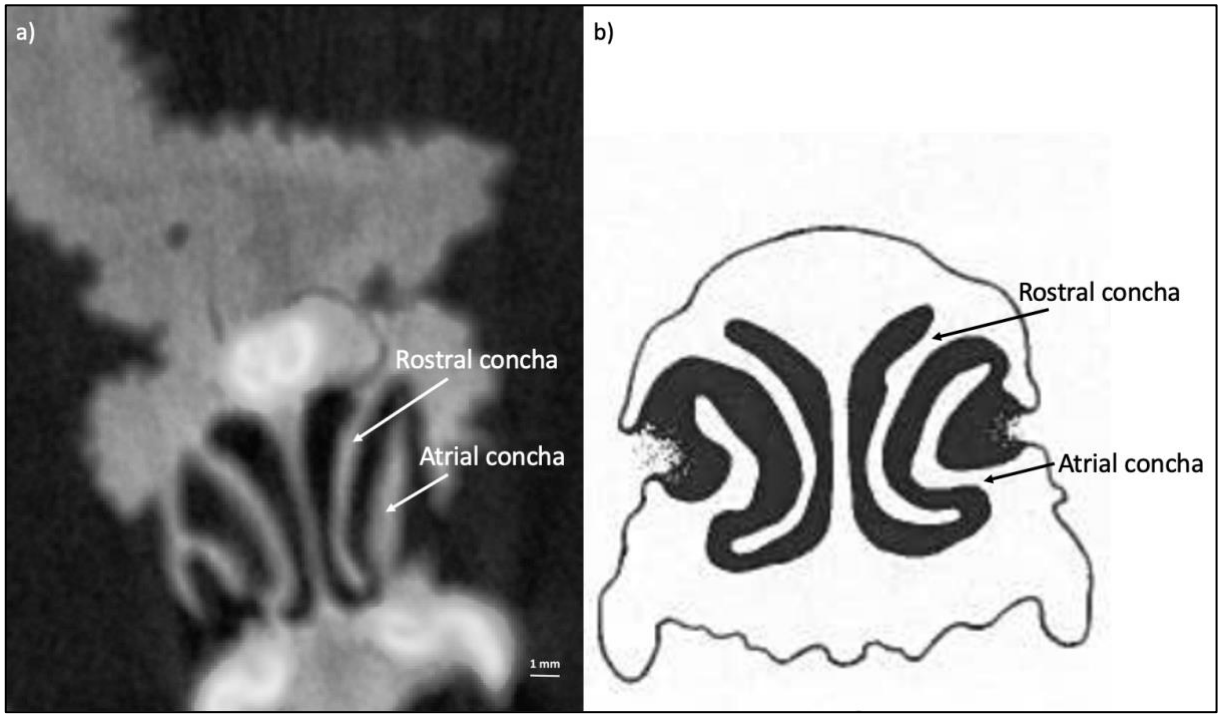

Figure 9: a) A CT image of the atrial and rostral conchae in the domestic chicken in the frontal plane. There is a greyscale spectrum from black to white, where black is air (least dense) and white is bone (most dense). Other tissues are in different shades of grey depending on their density. The image is oriented dorsal (top) to ventral (bottom). b) An illustration from Bang and Wenzel (1985, p. 201) of the atrial and rostral conchae in chicken. Air is black and white is tissue. The conchae marking is added by M. Westvik. No scale. The illustration is oriented dorsal (top) to ventral (bottom).

All ptarmigan species/subspecies had different shaped rostral conchae compared to the domestic chicken (Figure 10). The *crista nasalis* was difficult to identify in these different shaped rostral conchae. The presence of atrial conchae is unlikely as the shape and direction of the possible atrial conchae (Figure 10) differs from that of the chicken (Figure 9). Also, atrial conchae in chicken merged with the nasal cavity wall (Figure 11a), while the suspected atrial conchae in Svalbard rock ptarmigan merged with the rostral conchae (Figure 11b). This was also the case in rock and willow ptarmigan.

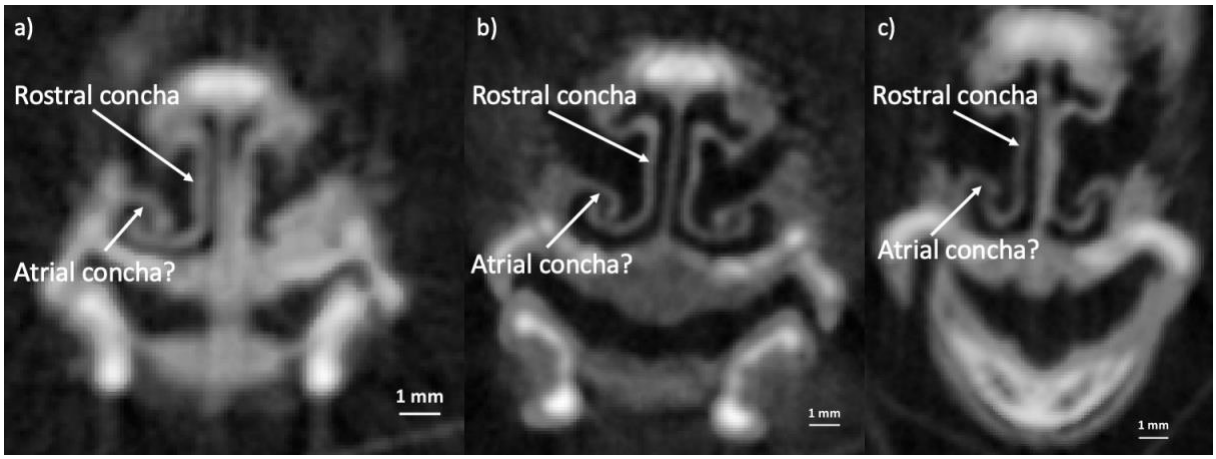

Figure 10: CT images of the rostral conchae in a) rock ptarmigan, b) Svalbard rock ptarmigan, and c) willow ptarmigan in the frontal plane. In both rock and willow ptarmigan the right rostral concha is collapsed giving it an appearance of being merged with the nasal septum. There is a greyscale spectrum from black to white, where black is air (least dense) and white is bone (most dense). Other tissues are in different shades of grey depending on their density. All images are oriented dorsal (top) to ventral (bottom).

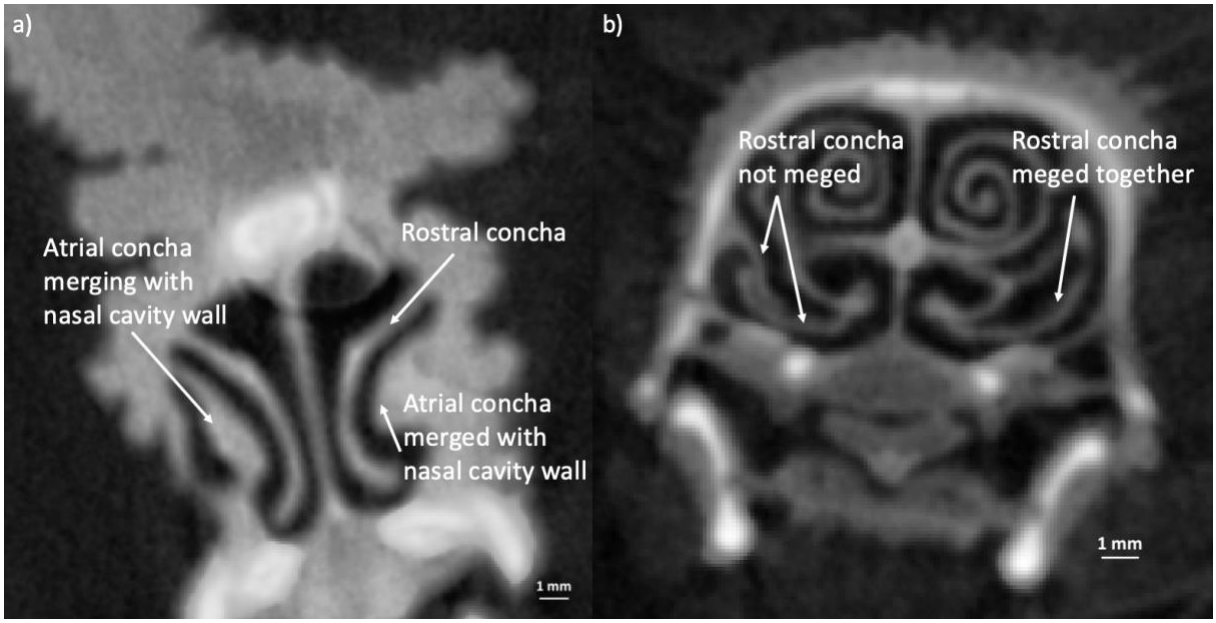

Figure 11: CT images of the a) atrial conchae in domestic chicken and b) rostral conchae in Svalbard rock ptarmigan in the frontal plane. Atrial conchae in chicken merged with the nasal cavity wall, while the suspected atrial conchae in Svalbard rock ptarmigan did not. There is a greyscale spectrum from black to white, where black is air (least dense) and white is bone (most dense). Other tissues are in different shades of grey depending on their density. Both images are oriented dorsal (top) to ventral (bottom).

3.2.1 Histology of rostral conchae

As for the histology, the rostral conchae consisted of hyaline cartilage covered by a *lamina propria* (a collagenous connective tissue) with an outer keratinized stratified squamous epithelium facing the air flow (Figure 12a). This means that the outer epithelium consists of several layers of cells with the basement layer being squamous (flattened) cells (Young et al., 2006). The epithelium ranged between 20 and 25 μm in thickness all around the rostral

conchae, while the *lamina propria* ranged between 10 μm in the thinnest places to 70 μm in the thickest places. As for the vascularization, there were some visible blood vessels scattered in the *lamina propria*, both arterioles and venules (Figure 12a). Arteries and arterioles have walls with more elastic and smooth muscle components and thereby a smaller lumen. Veins and venules have less elastic and smooth muscle components, thereby being thinner walled with a larger lumen. There are often less erythrocytes residing in the arteries and arterioles compared to the veins and venules (Young et al., 2006). However, the head specimen used for histology was not perfusion fixated. This means that the blood vessels are rinsed with for example physiological saline before a fixative like PFA is injected (e.g., Barroso, 2014). In that manner the natural diameter of the vessel will be preserved, rather than the flattened shape most of them take on now. Hence, only the larger arteries and veins were possible to identify in these histological slides (e.g., Figure 15a). Arterioles and venules were difficult to identify as they could be mistaken for cracks in tissue separation (Figure 12a).

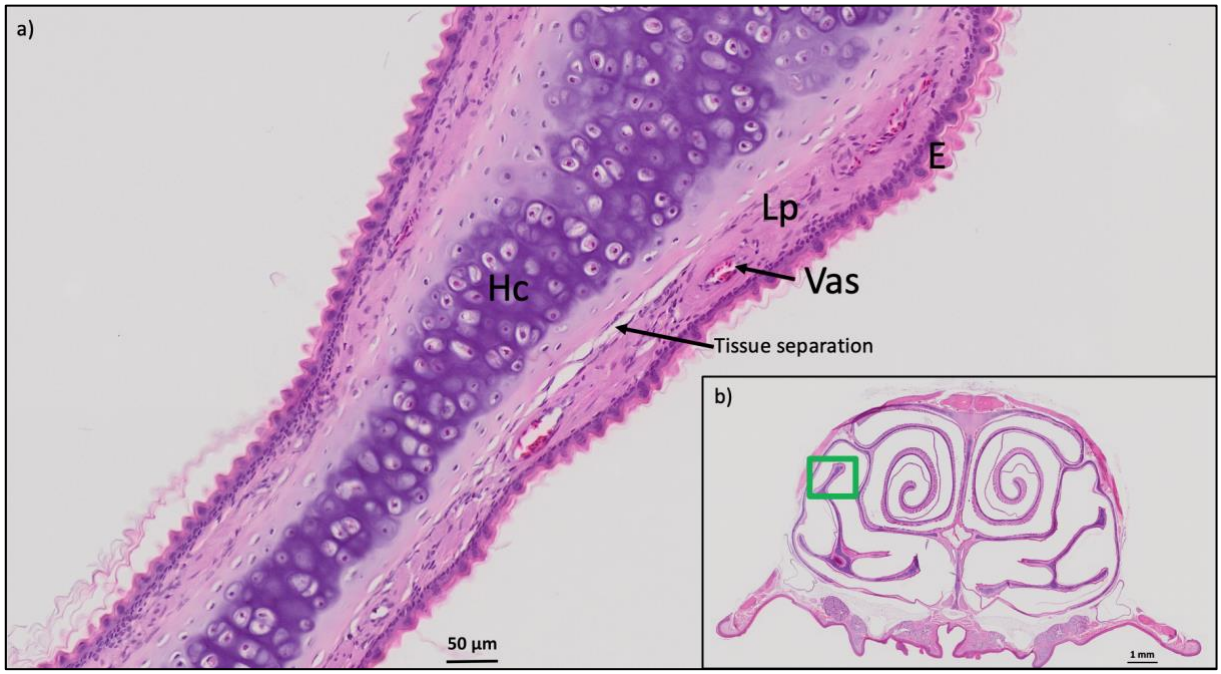

Figure 12: Histology of rostral conchae. a) A part of the rostral concha in Svalbard rock ptarmigan. It consists of hyaline cartilage (Hc), covered by lamina propria (Lp), and keratinized stratified squamous epithelium (E) all around. There are traces of vascularization (Vas) visible due to the red-stained erythrocytes. An example of tissue separated from the cartilage is also shown. b) Key to where on the rostral concha the image in a) is taken from.

3.3 Middle conchae

The middle conchae took on a scrolled shape for all study species, as seen in Figure 13. They protruded from each outer lateral nasal cavity wall and were a separated entity from the rostral conchae. At maximum scrolling the extended lengths of the middle conchae, scaled to

volume of air space, were 0.010 for chicken, 0.033 for Svalbard rock ptarmigan and 0.049 for willow ptarmigan.

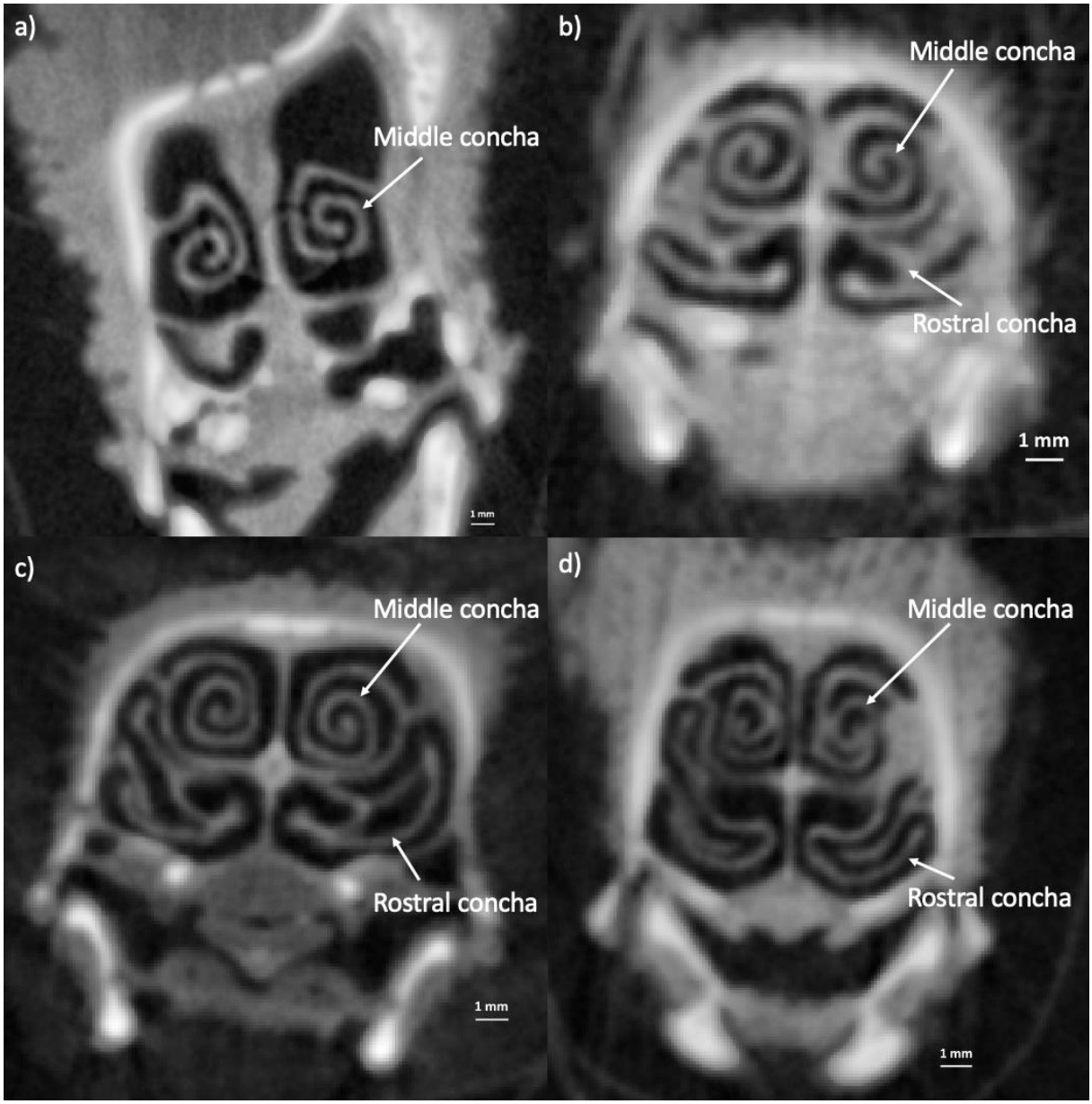

Figure 13: CT images of the middle conchae in a) domestic chicken, b) rock ptarmigan, c) Svalbard rock ptarmigan, and d) willow ptarmigan in the frontal plane. There is a greyscale spectrum from black to white, where black is air (least dense) and white is bone (most dense). Other tissues are in different shades of grey depending on their density. All images are oriented dorsal (top) to ventral (bottom). Examples are taken from where the scrolling was at or near maximum.

3.3.1 Histology of middle conchae

The middle conchae consisted, like the rostral conchae, of hyaline cartilage covered by a *lamina propria*, but they had an outer layer of pseudostratified columnar ciliated epithelium (respiratory epithelium) facing the air flow (Figure 14a). In respiratory epithelium all cells rest on the same basement membrane and take on a more columnar shape of varying lengths

as opposed to stratified squamous epithelium with flattened cells. As the name suggests, the cells are ciliated (Young et al., 2006). Individual goblet cells or larger gatherings of them (multicellular intraepithelial glands; mucus glands) were embedded in the respiratory epithelium, presumably producing mucus and keeping the conchae moist (Figure 14a). The respiratory epithelium ranged from about 20 μm in the thinnest places to about 110 μm in the thickest places, with the largest mucus glands being about 100 μm long. The variation in thickness also applies to the *lamina propria*, it being about 15 μm in the thinnest places and about 100 μm in the thickest places. In general, the *lamina propria* and the respiratory epithelium were thinner on the inside of the scroll (the concave surface) and thicker on the outside of the scroll (the convex surface), as seen in Figure 14a.

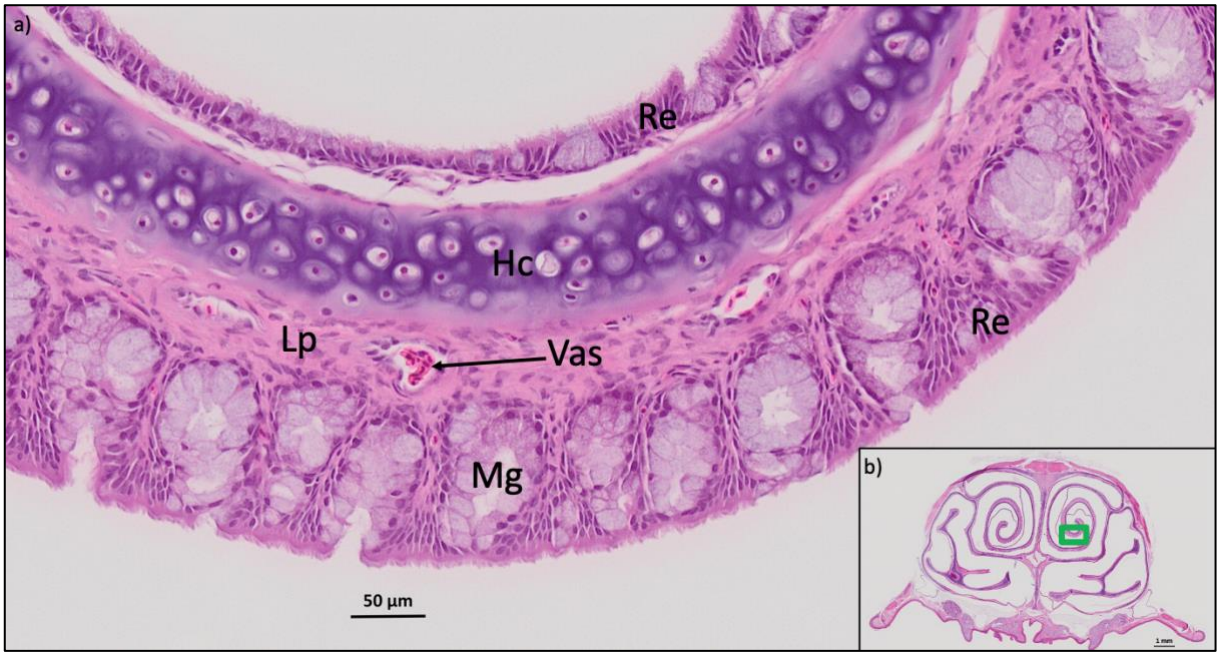

Figure 14: Histology of middle conchae. a) A part of the middle concha in Svalbard rock ptarmigan. It consists of hyaline cartilage (Hc), covered by lamina propria (Lp) and respiratory epithelium (Re) all around. The respiratory epithelium contains many mucus glands (Mg). There are visible blood vessels (Vas) due to the red-stained erythrocytes. b) Key to where on the middle concha the image in a) is taken from.

Large arteries were found at the top and in the middle part of the nasal septum wall, in the palate and where the middle conchae were attached to the lateral nasal cavity wall (Figure 15a). Veins were found close to the arteries. Hence, they appeared in bundles near each other, mostly arranged in the same direction as the air flow. A majority of the red-stained erythrocytes were found in the veins, while the arteries had few if any erythrocytes.

Figure 15: Histology of visible arteries and veins. a) An example of an artery (A) and two veins (V) located in the mucosal wall of the nasal septum. The thick-walled artery has fewer erythrocytes in its smaller lumen compared to the thinner walled veins. b) Key to where on the histological slide the image in a) is taken from.

3.4 Caudal conchae

The caudal conchae were similar in shape for all study birds (Figure 16). They were, together with the atrial conchae, the simplest of them all in having no scrolls but simply an outward-facing curved surface. They did, like the middle conchae, protrude from the lateral nasal cavity wall.

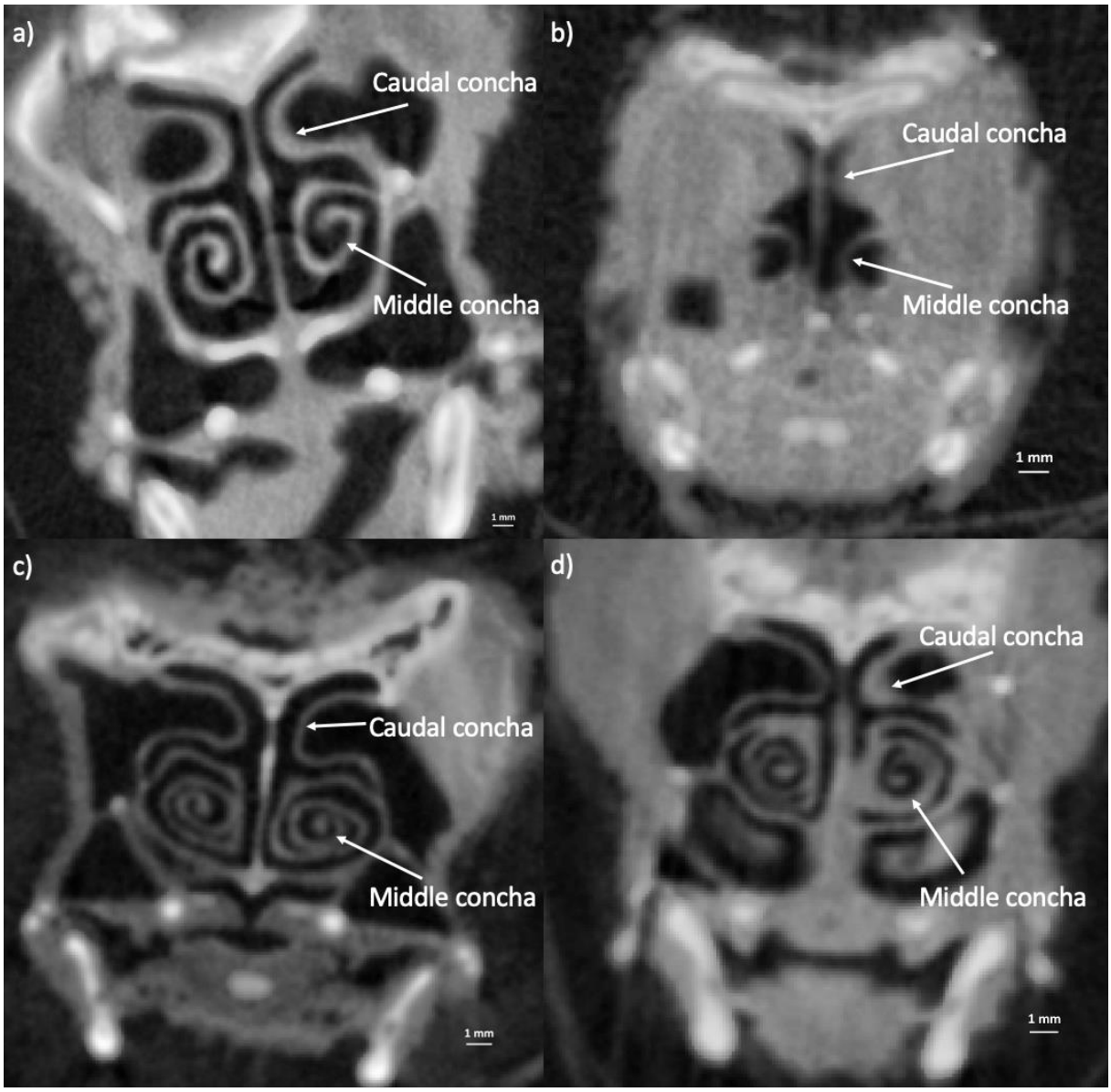

Figure 16: CT images of the caudal conchae in a) domestic chicken, b) rock ptarmigan, c) Svalbard rock ptarmigan, and d) willow ptarmigan in the frontal plane. There is a high degree of collapsed tissue in the rock ptarmigan specimen, reducing the contrast between air and tissue. There is a greyscale spectrum from black to white, where black is air (least dense) and white is bone (most dense). Other tissues are in different shades of grey depending on their density. All images are oriented dorsal (top) to ventral (bottom).

As the nasal cavity approached an end, respiratory epithelium covered the whole inside of the nasal cavity (Figure 17a). The middle conchae were still present, though in a very reduced state.

Figure 17: a) A histological section of the middle conchae at the caudal end of the nasal cavity in the frontal plane. The whole inside cavity is covered by respiratory epithelium. Parts of the orbits are in the top left and right corners. Oriented dorsal (top) to ventral (bottom). b) Key to were on the histological slide the image in a) is taken from.

3.5 Respiratory heat loss

The theoretical daily resting heat loss rates of a hypothetical 1 kg Svalbard rock ptarmigan were estimated to illustrate the potential importance of NHE in heat conservation. Firstly, V_{min} was calculated with Equation 1:

$$V_{min} = 386 * 1^{0.72} = 386\ mL/min = 0.386\ L/min$$

Next, the water vapour pressures (P_{wx}) at temperatures T_x = -10 °C, 20 °C and 40 °C were calculated with Equation 2. Calculations and conversions for T_a = -10 °C are shown in full:

$$P_{w10} = 6.112e^{\frac{17.67*(-10°C)}{(-10°C)+243.5}} = 2.868\ hPa$$

$$2.868\ hPa * 100 * 0.0075\ mmHg/Pa = 2.15\ mmHg$$

$$P_{w20} = 23.37\ hPa \Rightarrow 17.53\ mmHg$$

$$P_{w40} = 73.95\ hPa \Rightarrow 55.46\ mmHg$$

The amount of water inhaled (W_a) or lost (W_b or W_e) in V_{min} at the respective temperatures (T_x) were calculated with Equation 3. Calculations for T_a = -10 °C are shown in full:

$$W_a = \frac{0.622 * 2.15\ mmHg}{760\ mmHg - 2.15\ mmHg} * 0.001225\ kg/L * 10^6\ mg/kg * 0.386\ L/min = 0.83\ mg/min$$

$$W_b = 23.15\ mg/min$$

$$W_e = 6.94\ mg/min$$

Finally, the total amount of heat added upon inhalation, both as dry and evaporative heat, was calculated with Equation 4. It was assumed that all heat added to inhaled air at T_a = -10 °C is lost if the Svalbard rock ptarmigan is not able to recover respiratory heat and water. Hence, this value will be the same for T_e = 40 °C. Calculations of the amount of heat added at T_a = -10 °C are shown below:

$$Heat_{added} = \left(\left(\frac{0.386\ L/min}{60\ s/min}\right) * 10^3 J/°C/kg * \left(40°C - (-10°C)\right) * 0.001225\ kg/L\right) + \left(\frac{23.15\ mg/min - 0.83\ mg/min}{60\ s/min} * 2.34\ J/mg\right) = 1.26\ J/s\ = 1.26\ W$$

Heat lost if T_e = 20 °C was calculated with Equation 5:

$$Heat_{lost} = \left(\left(\frac{0.386\ L/min}{60\ s/min}\right) * 10^3 J/°C/kg * \left(20°C - (-10°C)\right) * 0.001225\ kg/L\right) + \left(\frac{6.94\ mg/min - 0.83\ mg/min}{60\ s/min} * 2.34\ J/mg\right) = 0.47\ J/s = 0.47\ W$$

Dividing these two numbers by the hypothetical weight (1 kg), showed that 1.26 W/kg is needed to heat air from -10 °C to 40 °C. Consequently, the same amount of heat is lost if the bird does not conserve any heat or water upon exhalation, i.e., T_e = 40 °C. 0.47 W/kg is lost if T_e = 20 °C and NHE is conserving heat and water. The respiratory heat conserved (%) is calculated as follows:

$$Respiratory\ heat\ conserved = 100\ \% - \left(\frac{0.47\ W/kg}{1.26\ W/kg} * 100\ \%\right) = 62.7\ \%$$

RMR from Mortensen and Blix (1986) for a 0.705 kg winter-acclimated Svalbard rock ptarmigan was 85.3 kcal/kg*day. This was converted to W/kg where 1 kcal = 4187 J:

$$RMR_{converted} = \frac{85.3\ kcal/kg * day * 4187\ J/kcal}{24\ t * 60\ min/t * 60\ s/min} = 4.13\ W/kg$$

From Nord and Folkow (2018), early winter RMR for Svalbard rock ptarmigan (>2yrs old birds) was 4.64 W/kg. A mean of these two RMRs is 4.39 W/kg. The proportion of RMR that was lost assuming efficient NHE (T_e = 20 °C) or no NHE (T_e = T_b = 40 °C) were calculated:

$$\%\ heat\ of\ RMR, with\ NHE = \frac{0.47\ W/kg}{4.39\ W/kg} * 100\ \% = 10.7\ \%$$

$$\%\ heat\ of\ RMR, without\ NHE = \frac{1.26\ W/kg}{4.39\ W/kg} * 100\ \% = 28.7\ \%$$

The % differences in how much energy that was lost with and without NHE were used to calculate the energy savings resulting from employing NHE:

$$\%\ reducion\ of\ RMR = 28.7\ \% - 10.7\ \% = 18.0\ \%$$

All these hypothetical values are summarized and illustrated in Figure 18.

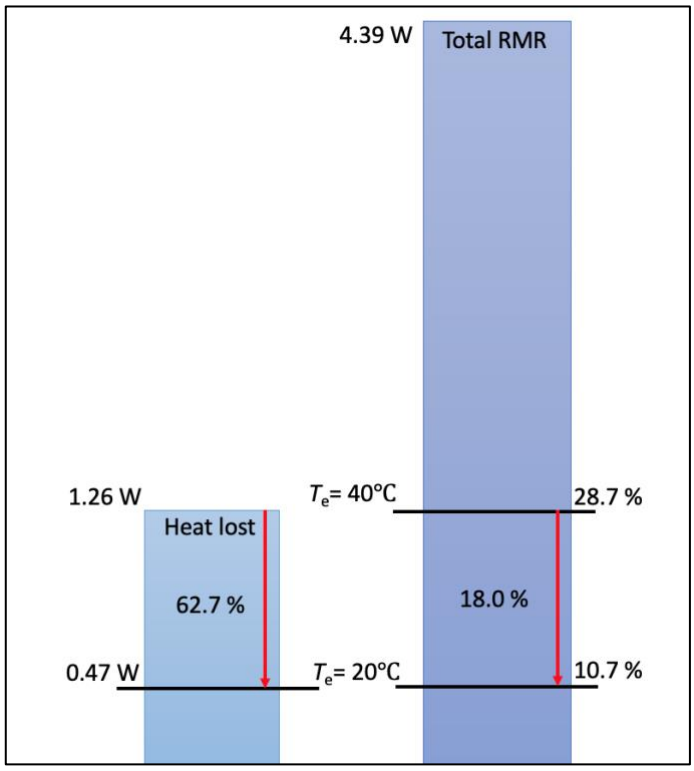

Figure 18: A schematical illustration of the heat losses when NHE is employed and when it is not. Respiratory heat loss is reduced by 62.7 % with NHE (T_e = 20 °C, left histogram bar), and this corresponds to an 18 % reduction of total RMR (right histogram bar).

4 Discussion

Firstly, general differences between the study birds will be discussed. This is followed by more specific discussions on each concha, atrial and rostral, middle and caudal respectively, before the potential importance of NHE in reducing respiratory heat loss is addressed.

4.1 Habitat adaptation among the study birds

The Svalbard rock ptarmigan had the largest conchal surface area independent of body size differences between the study birds (Table 2 and Figure 7d). The willow ptarmigan had the largest conchal surface area in relation to volume of air space, with the Svalbard rock ptarmigan being intermediate and the chicken having the smallest ratio (Table 3 and Figure 8). Danner et al. (2017) found that a desert-adapted subspecies of songbirds had larger conchae in larger nasal cavities than a subspecies inhabiting moister temperate areas. Water conservation in the dry habitat was concluded to be the main driver behind this adaptation, the larger nasal cavities allowing for larger conchae and subsequently greater water conservation. On the contrary, Mason et al. (2020) concluded that heat conservation was the main driver behind turbinate divergence in phocid seals adapted to tropical, temperate and polar habitats. Conchal size could therefore be a result of either heat or water conservation, or both. In this case heat retention is probably the main driver.

The overlap between rostral and middle conchae were greater in Svalbard rock and willow ptarmigan compared to the domestic chicken (Figure 7a-c). This was also the case in the two songbird subspecies adapted to different habitats, the desert-adapted subspecies having greater overlap than the temperate adapted one (Danner et al., 2017). All bird specimens used in this thesis originated from birds raised in the same county. This suggests that they had been raised under similar climatic conditions, but with possible local variation. Even though the Svalbard rock ptarmigan had the greatest absolute conchal surface area independent of scaling (Figure 7d), the willow ptarmigan exceeded the Svalbard rock ptarmigan when scaled to volume of air space (Figure 8). The Gulf Stream provides warmer waters to the west coast of Svalbard, which causes a milder climate than what it could have been considering the high latitudinal location (Norderhaug, 1984). The cold-temperate climate in Indre Troms could be borderline to polar (Beck et al., 2018), which means that all ptarmigan species/subspecies could have adapted to very similar habitats. This could explain the similarities between the Svalbard rock and willow ptarmigan conchae found in this thesis. Potentially, adaptation to habitat have happened in both species, thus using specimens from warm-temperate habitats

either along the coast or further south in Norway could be an option to better investigate for conchal differences. The domestic chicken, coming from a local breeder, can escape the worst cold by remaining inside the (possibly heated) hen house. Being fed and having constant access to water could therefore reduce its need for heat and water conservation structures.

Evolutionary adaption to habitat is not the only possible explanation for more elaborate conchae in polar and cold-temperate adapted bird species. Phenotypic plasticity, that is the expression of different phenotypes in response to changing environmental conditions, could also be an explanation (Fusco & Minelli, 2010). For example, Midtgård (1989c) found that the temperate-adapted herring gulls (*Larus argentatus*) had similar vascularization and AVA density in the feet, eyelids and nasal mucosa compared to the polar-adapted Iceland gulls (*Larus glaucoides*). Midtgård (1989c) suggested that both species of gulls had been subjected to sub-zero temperatures, and therefore had similar vascularization. Hence, acclimatization to local temperature variation could affect the development of microanatomical structures important for heat exchange. Furthermore, Midtgård (1989c) concluded that the Iceland gull had a more efficient heat exchanger in their feet compared to the herring gull. Potentially, evolutionary adaptation to habitat resulted in more specialized structures for heat exchange in the polar-adapted Iceland gull as opposed to the temperate herring gull, or this could be a result of phenotypic plasticity. Hence, local variations in temperature and other environmental factors must therefore be taken into account when choosing study birds, but also when setting up an experimental study. Past climatic conditions that the study birds were exposed to could therefore have affected the results obtained in this thesis, if for example the climate was unusually cold in Indre Troms and at the same time unusually warm in Tromsø.

The Svalbard rock and willow ptarmigan had smaller nasal cavities than the chicken, but larger or almost equally sized conchae (Table 2). The larger conchae could therefore potentially reduce the distance between the centre of the air flow and the mucosal surfaces, being two of the four factors that affects the effectiveness of NHE (Murrish & Schmidt-Nielsen, 1970). Body size differences between the study birds are not considered as original body mass is lacking (Table 1), but then body mass is not necessarily the best scaling variable. For example, turbinal surface area in carnivores are smaller in lager species, possibly because of greater body volume to surface area ratio and slower respiration rates. Heat dissipation and respiratory water losses would subsequently be lower, and the need for elaborate turbinates would not be as crucial (Van Valkenburgh et al., 2011). Comparing conchal size between equally sized and closely related species/subspecies of birds could

therefore be important for future studies on this topic. This thesis was based on already existing specimen availability of both wild and captive birds, from both scientific and private origin. Hence, the limited existing material was used on an opportunistic basis as the Svalbard rock ptarmigan are valuable experimental birds and not available in unlimited supply.

4.2 Atrial and rostral conchae

Atrial conchae are, as far as literature goes, only present in some Galliform birds, the domestic chicken being the best-known example (Bang, 1971). However, there seems to be no further records of why atrial conchae in domestic chicken should be regarded as a separate entity from rostral conchae. From analyses of the CT images, atrial conchae were completely separated entities from the rostral conchae in the domestic chicken. They merged with the lateral nasal cavity wall (Figure 11a). This is in accordance with findings from Watanabe et al. (2020) on chicken. For the Svalbard rock ptarmigan, the possible atrial conchae merged with the rostral conchae (Figure 11b), which was also the case in rock and willow ptarmigan. This suggests that the ptarmigan species/subspecies have more elaborate rostral conchae than presence of atrial conchae. Rostral conchae shape have been found to vary between unrelated bird species (Bang & Wenzel, 1985), and their size has also been found to vary among songbird subspecies adapted to different habitats (Danner et al., 2017). According to Table 2, the rostral conchae were larger in both Svalbard rock and willow ptarmigan compared to the chicken when scaled to volume of air space. Hence, despite the lack of atrial conchae, the ptarmigan species/subspecies have more well-developed rostral conchae than the domestic chicken.

The rostral conchae had a cartilaginous centre covered by a *lamina propria* and keratinized stratified squamous epithelium as a surface layer (Figure 12a). This is a continuation of the keratinized outer skin, which is also the case in domestic chicken (Bang, 1971; Watanabe et al., 2020), wild turkey (Bourke & Witmer, 2016) and greylag goose (*Anser anser*; order Anseriformes) (Harem et al., 2018). The keratinized epithelium could cause the white/light pink colour observed during the dissection (Figure 4c). No goblet cells or mucus glands were found here, and degree of vascularization was not possible to quantify due to reasons previously stated. However, Bang and Wenzel (1985) described a rich vascular bed in the *lamina propria* beneath the keratinized epithelium in chicken, which implies a possible thermoregulatory function despite its lack of respiratory epithelium. As suggested by Bang (1971), and later confirmed by Bourke and Witmer (2016), the rostral (and atrial) conchae are

important as airway baffles directing the airstream to specific parts of the nasal cavity. Rostral conchae direct the air flow over the *crista nasalis* (Figure 1), which works as a reservoir for secretions from the nasal gland (Bang & Wenzel, 1985). Hence, the air gets humidified as it passes over this part before it continues to the middle conchae. This could be important for protection of the respiratory epithelium in the middle conchae against very dry and cold inhaled air.

4.3 Middle conchae

The middle conchae were similar in general shape for all study birds (Figure 13). There were, however, length differences of these conchae between all study birds. Scaled to volume of air space, the willow ptarmigan had the longest middle conchae. Svalbard rock ptarmigan was intermediate, while the chicken had the shortest middle conchae. The rock ptarmigan specimen was not possible to analyse from the rostral end of the middle conchae. This could be a result of the CT scanner being out of service for about three months, the malfunctioning happening at the initial planned scan of the rock and willow ptarmigan specimen. The prepped heads were thereby thawed, frozen again at the PET Imaging Center before they were thawed a second time when the scanner had been fixed. The initial fluid clearing by flushing air through the nasal cavities was possibly counteracted by this. Even so, middle conchal surface area was larger in Svalbard rock and willow ptarmigan compared to the domestic chicken in relation to volume of air space (Table 3). This could be a result of adaptation to habitat, similar to the desert-adapted songbirds investigated by Danner et al. (2017) and the polar phocid seals investigated by Mason et al. (2020), or phenotypic plasticity.

The middle conchae, like the rostral conchae, consisted of hyaline cartilage covered by a *lamina propria* and respiratory epithelium facing the air flow (Figure 14a). Respiratory epithelium in grey seals was found to contain numerous mucus glands with a well vascularized *lamina propria* beneath (Folkow et al., 1988). Similar findings are documented in graylag goose (Harem et al., 2018). An artery : vein ratio of approximately 1:30 was found in the respiratory turbinates of grey seals (Folkow et al., 1988). Solberg et al. (2020) further investigated if this high proportion of veins vs. arteries, also observed in reindeer, were important for heat exchange in the nasal mucosa of reindeer. Their findings suggested that it is indeed important for maintaining the temperature gradient in the nasal mucosa so that heat dissipation is kept within limits. A perfusion fixation could be an alternative to investigate if

this skewed artery : vein ratio is also present in the nasal mucosa of all ptarmigan species/subspecies.

The difference in thickness of respiratory epithelium between the concave and convex surface (Figure 14a) is a general characteristic among middle conchae in birds (Owerkowicz et al., 2014), but also seen in reindeer turbinates (Barroso, 2014). This can be a result of their growth during development, the epithelium growing over the expanding and scrolling cartilage (Barroso, 2014; Hogan et al., 2020). The scrolled shape and variation in epithelial thickness could also be related to the pathway air takes when passing through these structures. Reducing the velocity and maximizing amount of air in contact with mucosal surfaces would facilitate NHE (Murrish & Schmidt-Nielsen, 1970). Digital modelled air flow models have been used to investigate for similar research questions in wild turkey (Bourke & Witmer, 2016) and reindeer (Solberg et al., 2020), and could therefore be an option to look for possible adaptation to habitat among closely related bird species. Furthermore, respiratory epithelium continued all the way until the caudal end of the cavity (Figure 17a), which is also observed in chicken (Watanabe et al., 2020). Hence, heat and water exchange continue the whole length of the nasal cavity.

4.4 Caudal conchae

Excluding the atrial conchae, the caudal conchae were the smallest of the three main conchae in all study birds (Table 2). Also known as olfactory conchae, these are naturally the place of olfaction and are therefore covered in olfactory epithelium (Bang, 1971). Even so, their existence and importance in birds were for long neglected and deprioritized in research (Bang, 1960). Yellow-coloured caudal conchae (Figure 4c) are a recurring trait among different orders of birds, some examples being rheas, loons and petrels (Bang, 1971). As previously mentioned, the rostral conchae direct the air flow around the *crista nasalis*, which also launches the air towards the caudal conchae in a turkey nose. The geometry of the caudal conchae reduces the air flow velocity, allowing more time for odorant molecules to bind to receptors (Bourke & Witmer, 2016).

Both Svalbard rock and willow ptarmigan had at least twice as large caudal conchae relative to volume of air space as compared to the domestic chicken (Table 3). Van Valkenburgh et al. (2011) found that some terrestrial carnivores had greater olfactory turbinate surface area than respiratory turbinate surface area, while the inverse was the case for phocid seals. Terrestrial carnivores like the wolverine depend on their sense of smell to locate prey, while underwater-

hunting seals must use other means to locate prey. Bang (1971) points out that Pelecaniformes (i.e., pelicans, shoebills, herons etc.) were amongst the birds that had the lowest calculated olfactory ratios among 23 different bird orders. Especially pelicans have a marine diet, thereby possibly reducing the need for olfaction to locate prey, like seals (Van Valkenburgh et al., 2011). Hence, caudal conchae can be more important in birds that have to locate their food by olfaction, like terrestrial predatory birds. Magpies (*Pica pica*; order Passeriformes) actively use olfaction to locate cached seeds and nuts (Molina-Morales et al., 2020). Hence, the sense of smell might be more important in the wild rock and willow ptarmigan to located food, compared to the domestic chicken having a fair amount supplied. This can be one explanation for the larger caudal conchae found in the ptarmigan species/subspecies compared to the domestic chicken, although the Svalbard rock ptarmigan had a captive origin.

4.5 Respiratory heat loss

The Svalbard rock ptarmigan is, as already mentioned, adapted to a hostile and harsh environment with low temperatures year-round and a scarcity of both food and light in the winter (Norderhaug, 1984). Any mode of energy conservation is therefore important for winter survival of this high-arctic residential bird, respiration and respiratory heat loss being addressed in this thesis. In this hypothetical example the Svalbard rock ptarmigan is resting in -10 °C, which is close to their lower critical temperature (Mortensen & Blix, 1986). As explained by Mortensen and Blix, the bird must increase its metabolic rate to keep a stable body core temperature if ambient temperature decreases further below this. Hence, all calculations are based on the bird not having an increased resting metabolism, just keeping a stable body core temperature by other physiological and behavioural means.

NHE potentially reduces the metabolic costs of respiration with 18.0 % of total RMR (Figure 18). These values are similar to results from Murrish (1973), where he found a 17 % potential reduction in the metabolic costs in Adélie penguins. Respiratory heat loss if air was exhaled at body core temperature was estimated to 20.4 % of total RMR for these penguins. For the Svalbard rock ptarmigan, this was estimated to be 28.7 % of RMR. The higher costs found in Svalbard rock ptarmigan could be a result of allometry and the higher mass-specific metabolic rates of smaller birds compared to larger ones (Bennett & Harvey, 1987). However, Murrish captured the penguins on the Antarctic Peninsula, which according to Beck et al. (2018), has an even harsher climate than Svalbard. Hence, Adélie penguins might therefore have adapted to have an even more efficient NHE than the Svalbard rock ptarmigan. This can be further

supported by the estimated respiratory savings. While the Svalbard rock ptarmigan recovered 62.7 % of the heat added upon inhalation during exhalation, Murrish (1973) estimated that the Adélie penguins could recover 83.4 % of the heat added upon inhalation during exhalation. Conchae adaptation to habitat, and thereby NHE efficiency, is one possible reason for this difference in respiratory heat savings. It should, however, be noted that the ambient air temperature in Murrish' experiments was 5 °C, compared to the lower hypothetical -10 °C used in this thesis. How the amount of energy saved with NHE would be affected if the lower critical temperature is passed and an increase the RMR happens would be an interesting aspect to further investigate by experimental studies.

Schmidt-Nielsen et al. (1970) estimated that the cactus wren (*Campylorhynchus brunneicapillus*; order Passeriformes), living in the dry southwestern American deserts, could conserve 75 % of the heat and 74 % of the water added upon inhalation during exhalation, at an ambient air temperature of 15 °C. The cactus wren used in this study, with a body mass of 35 g, is thereby a much smaller bird than the Svalbard rock ptarmigan. Hence, habitat adaptation of their conchae and efficient NHE for primarily water conservation can be a potential explanation for this higher conservation rate compared to the Svalbard rock ptarmigan. It is necessary to emphasize that both Murrish (1973) and Schmidt-Nielsen et al. (1970) had actual measurements of inhaled and exhaled temperature, while hypothetical values were used in this thesis as live experimental birds were not available. It would, however, be interesting to conduct such an experimental study on live rock, Svalbard rock and willow ptarmigan and measure exhaled air temperature and minute respiration at different ambient air temperatures to quantify heat losses and heat savings more precisely.

Respiratory heat loss was not modelled for any of the other study birds, as all values were hypothetical. As the Svalbard rock ptarmigan have more elaborate conchae than the domestic chicken, it follows that it also likely has a more efficient NHE. However, Schmidt-Nielsen et al. (1970) did not find much difference in exhaled air temperatures for birds inhabiting hot deserts vs. temperate habitats over an ambient temperature range from 10 to 30 °C. One could imagine that water conservation would be more important for the desert-adapted birds, which implies that their exhaled temperatures should be lower than the ones of the temperate birds. However, the birds used by Schmidt-Nielsen and colleagues were from different orders, among them a domestic duck (*Anas platyrhyncos domesticus*; order Anseriformes), a cactus wren and a domestic pigeon (*Columba livia domestica*; order Columbiformes). Birds from these orders use different mechanisms to cope with excessive heat loads (Smith et al., 2017),

the cactus wren using energy-demanding panting as opposed to more efficient gular fluttering in the domestic pigeon. Such interspecies differences must be considered when addressing the efficiency of NHE, thereby using closely related species that use similar regulating mechanisms. Furthermore, desert-adapted birds are normally subjected to year-round higher temperatures than temperate-adapted birds (Beck et al., 2018). Potentially, exposing temperate and desert birds to temperatures between 20 to 50 °C could be a way to test if there are differences in the efficiency of NHE. At these temperatures heat dissipation could be in conflict water conservation, and the conchae of desert-adapted birds might be better adapted to deal with this dilemma than them of temperate birds.

The trachea could also be a potential place for heat and water exchange, however, measured temperature gradients within the nasal cavity of other birds show that close to all of the heat exchange happens in the nasal cavity (Geist, 2000; Murrish, 1973; Schmidt-Nielsen et al., 1970). Furthermore, Geist (2000) found that temperate-adapted nasal breathing birds recovered more heat and water compared to mouth breathing birds with conchae experimentally bypassed, at an ambient temperature of 15 °C. The trachea is therefore presumably not important in heat and water exchange, while NHE is an efficient physiological mechanism for heat and water conservation in avian respiration, regardless of habitat.

Skog and Folkow (1994) showed that temperature of exhaled air in grey seals did not change in response to manipulations of their water balance. Together with the findings from Mason et al. (2020), where tropical seals had smaller and less elaborate turbinates than their polar relatives, we can probably conclude that the need for heat retention is what favours turbinate size, at least in areas where water is not a constraining factor. While this is the case in seals, and supposedly other mammals as well (Owerkowicz et al., 2014), the evidence is not as clear for avian taxa. For now, conchae size seems to be linked to heat retention in cold habitats (e.g., this thesis), and to water retention in warmer habitats (Danner et al., 2017). There is a predominance of studies done on mammalian turbinates as opposed to avian conchae, which must be considered. Previous research on nasal conchae in birds have been conducted in various ways, using many different methods to investigate the complexity and function of them (e.g., Danner et al., 2017; Geist, 2000; Schmidt-Nielsen et al., 1970). With the recent technological advancements, an integrated analysis of breathing rates, actual measured heat- and water losses (or temperatures), anatomical structure and digital modelled air flow could improve our understanding of the functional physiology of avian nasal conchae.

5 Conclusion

Svalbard rock and willow ptarmigan had larger conchae compared to the domestic chicken, in relation to volume of air space in the nasal cavities. This implies that more air can be in contact with the mucosal surfaces at any given time point, thereby facilitating a more efficient heat and water exchange. Heat conservation is likely the main driver for this in the polar and cold-temperate adapted ptarmigan species/subspecies. NHE potentially reduces the daily metabolic costs by 18 % of total RMR in a hypothetical Svalbard rock ptarmigan case, which is similar to findings on other cold-adapted birds. Thus, there are indications for an evolutionary adaptation to habitat among the polar and cold-temperate adapted ptarmigan species. However, possible phenotypic plasticity and exposure to past climatic variations are important to consider when addressing these types of research questions. Future research should have an integrated approach to understand the functional anatomy and physiology of nasal conchae in birds adapted to different habitats, including experimentation on live birds during exposure to various thermal conditions.

References

Angilletta, M. J., Cooper, B. S., Schuler, M. S., & Boyles, J. G. (2010). The evolution of thermal physiology in endotherms. *Front Biosci, 2*, 861-881.

Bang, B., & Wenzel, B. (1985). Nasal cavity and olfactory system. In A. S. King & J. McLelland (Eds.), *Form and Function in Birds* (Vol. 3, pp. 195-225). Academic Press.

Bang, B. G. (1960). Anatomical Evidence for Olfactory Function in Some Species of Birds. *Nature*, *188*(4750), 547-549. https://doi.org/10.1038/188547a0

Bang, B. G. (1971). Functional anatomy of the olfactory system in 23 orders of birds. *Acta. Anat., 79*, 1-76.

Barroso, I. (2014). *The ontogeny of nasal heat exchange structures in Arctic artiodactyles* [MSc, UiT].

Batkowska, J., Brodacki, A., Zięba, G., Horbańczuk, J. O., & Łukaszewicz, M. (2015). Growth performance, carcass traits and physical properties of chicken meat as affected by genotype and production system. *Arch Anim Breed*, *58*(2), 325-333. https://doi.org/10.5194/aab-58-325-2015

Baumel, J. J., King, A. S., Breazile, J. E., Evans, H. E., & Berge, J. C. V. (Eds.). (1993). *Handbook of Avian Anatomy: Nomina Anatomica Avium* (2 ed.). Nuttall Ornithological Club.

Beck, H. E., Zimmermann, N. E., McVicar, T. R., Vergopolan, N., Berg, A., & Wood, E. F. (2018). Present and future Köppen-Geiger climate classification maps at 1-km resolution. *Sci Data*, *5*, 180214. https://doi.org/10.1038/sdata.2018.214

Bennett, P. M., & Harvey, P. H. (1987). Active and resting metabolism in birds: allometry, phylogeny and ecology. *J Zool*, *213*, 327-363.

Blix, A. S., & Johnsen, H. K. (1983). Aspects of nasal heat exchange in resting reindeer. *J Physiol*, *340*(1), 445-454.

Bolton, D. (1980). The Computation of Equivalent Potential Temperature. *Monthly weather review*, *108*(7), 1046-1053.

Bourke, J. M., & Witmer, L. M. (2016). Nasal conchae function as aerodynamic baffles: Experimental computational fluid dynamic analysis in a turkey nose (Aves: Galliformes). *Respir Physiol Neurobiol*, *234*, 32-46. https://doi.org/10.1016/j.resp.2016.09.005

Brekke, M., Kolbenstvedt, A., & Borthne, A. (2022, 26th Apr). CT. In *Store medisinske leksikon*. https://sml.snl.no/CT.

Cole, P. (1954). Recordings of respiratory air temperature. *J Laryngol Otol*, *68*, 295-307.

Cromey, D. W. (2010). Avoiding Twisted Pixels: Ethical Guidelines for the Appropriate Use and Manipulation of Scientific Digital Images. *Sci Eng Ethics*, *16*(4), 639-667. https://doi.org/10.1007/s11948-010-9201-y

Danner, R. M., & Greenberg, R. (2015). A critical season approach to Allen's rule: bill size declines with winter temperature in a cold temperate environment. *J. Biogeogr*, *42*(1), 114-120. https://doi.org/10.1111/jbi.12389

Danner, R. M., Gulson-Castillo, E. R., James, H. F., Dzielski, S. A., Frank, D. C., Sibbald, E. T., & Winkler, D. W. (2017). Habitat-specific divergence of air conditioning structures in bird bills. *The Auk*, *134*(1), 65-75. https://doi.org/10.1642/AUK-16-107.1

Darwin, C. (1882). *On the Origin of Species* (6th ed.). Apple Books.

Dyck, J. (1979). Winter plumage of the rock ptarmigan: Structure of the air filled barbules and function of the white color. *Dansk Orn Foren Tidsskr*, *73*(1-2), 41-58.

Folkow, L. P. (1992). Adrenergic vasomotor responses in nasal mucosa of hooded seals. *Am J Physiol*, *263*(6), 1291-1297. https://doi.org/10.1152/ajpregu.1992.263.6.R1291

Folkow, L. P., Blix, A. S., & Eide, T. J. (1988). Anatomical and functional aspects of the nasal mucosal and ophthalmic retia of phocid seals. *J Zool Lond*, *216*(3), 417-436. https://doi.org/10.1111/j.1469-7998.1988.tb02439.x

Frappell, P. B., Hinds, D. S., & Boggs, D. F. (2001). Scaling of Respiratory Variables and the Breathing Pattern in Birds: An Allometric and Phylogenetic Approach. *Physiol Biochem Zool*, *74*(1), 75-89. https://doi.org/10.1086/319300

Fusco, G., & Minelli, A. (2010). Phenotypic plasticity in development and evolution: facts and concepts. *Philos Trans R Soc Lond B Biol Sci*, *365*(1540), 547-556. https://doi.org/10.1098/rstb.2009.0267

Gamble, M., & Bancroft, J. D. (2008). Bone. In *Theory and practice of histological techniques* (6th ed., pp. 333-364). Churchill Livingstone Elsevier.

Geist, N. R. (2000). Nasal Respiratory Turbinate Function in Birds. *Physiol Biochem Zool*, *73*(5), 581-589. https://doi.org/10.1086/317750

Harem, İ., Kocak, M., & Sari, E. K. (2018). The histological structure and histochemistry of the mucosa of the nasal conchae in geese, Anser anser. *Biotech Histochem*, *93*(6), 432-441. https://doi.org/10.1080/10520295.2018.1450523

Hillenius, W. J. (1992). The Evolution of Nasal Turbinates and Mammalian Endothermy. *Paleobiology*, *18*(1), 17-29. https://doi.org/10.1017/S0094837300012197

Hogan, A. V., Watanabe, A., Balanoff, A. M., & Bever, G. S. (2020). Comparative growth in the olfactory system of the developing chick with considerations for evolutionary studies. *J Anat*, *237*(2), 225-240.

Høst, P. (1942). Effect of light on the moult and sequences of plumage in the willow ptarmigan. *The Auk*, *59*, 388-403.

Huntley, A. C., Costa, D. P., & Rubin, R. D. (1984). The contribution of nasal countercurrent heat exchange to water balance in the northern elephant seal, Mirounga angustirostris. *J Exp Biol*, *113*, 447-454.

Hussein, I., Raad, M., Safa, R., Jurjus, R. A., & Jurjus, A. (2015). Once upon a microscopic slide: the story of histology. *J Cytl Histol*, *6*(6), 1-4. https://doi.org/10.4172/2157-7099.1000377

International Committee on Veterinary Gross Anatomical Nomenclature (Ed.). (2017). *Nomina Anatomica Veterinaria* (6 ed.). World Association of Veterinary Anatomists.

Irving, L., & Krog, J. (1954). Body temperatures of arctic and subarctic birds and mammals. *J Appl Physiol*, *6*(11), 667-680. https://doi.org/10.1152/jappl.1954.6.11.667

Jackson, D., & Schmidt-Nielsen, K. (1964). Countercurrent heat exchange in the respiratory passages. *Proc natn Acad Sci*, *51*, 1192-1197.

Johnsen, H. K., Blix, A. S., Jørgensen, L., & Mercer, J. B. (1985). Vascular basis for regulation of nasal heat exchange in reindeer. *Am J Physiol*, *249*(5), 617-623. https://doi.org/10.1152/ajpregu.1985.249.5.R617

Kiernan, J. A. (2008). Decalcification and other treatments for hard tissues. In *Histological and histochemical methods: theory and practice* (4th ed., pp. 45-51). Scion.

Kuehnel, W. (2003). *Color atlas of cytology, histology, and microscopic anatomy* (4th ed.). Thieme.

Lasiewski, R. C., & Calder, W. A. (1971). A preliminary allometric analysis of respiratory variables in resting birds. *Respiration Physiology*, *11*(2), 152-166. https://doi.org/10.1016/0034-5687(71)90020-X

Lees, J., Nudds, R., Stokkan, K.-A., Folkow, L., & Codd, J. (2010). Reduced Metabolic Cost of Locomotion in Svalbard Rock Ptarmigan (Lagopus muta hyperborea) during Winter. *Plos One*, *5*(11), e15490-e15490. https://doi.org/10.1371/journal.pone.0015490

Lindgård, K., Naslund, S., & Stokkan, K. A. (1995). Annual changes in body mass in captive Svalbard ptarmigan: role of changes in locomotor activity and food intake. *J Comp Physiol B*, *165*(6), 445-449. https://doi.org/10.1007/BF00261298

Løvenskiold, H. L. (1954). *Skrifter Nr. 103. Studies on the avifauna of Spitsbergen.* Norwegian Polar Institute.

Løvenskiold, H. L. (1964). *Skrifter nr. 129. Avifauna Svalbardensis: with a discussion on the geographical distribution of the birds in Spitsbergen and adjacent islands*. Norwegian Polar Institute.

Mason, M. J., Wenger, L. M. D., Hammer, Ø., & Blix, A. S. (2020). Structure and function of respiratory turbinates in phocid seals. *Polar Biol*, *43*, 157-173. https://doi.org/10.1007/s00300-019-02618-w

Midtgård, U. (1989a). Development of arteriovenous anastomoses in the skin of the chicken and the influence of environmental temperature. *Am J Anat*, *186*(3), 300-305. https://doi.org/10.1002/aja.1001860306

Midtgård, U. (1989b). The effect of heat and cold on the density of arteriovenous anastomoses and tissue composition in the avian nasal mucosa. *Journal of Thermal Biology*, *14*(2), 99-102.

Midtgård, U. (1989c). A morphometric study of structures important for cold resistance in the arctic iceland gull compared to herring gulls. *Comp Biochem Physiol part A*, *93*(2), 399-402. https://doi.org/10.1016/0300-9629(89)90055-8

Molina-Morales, M., Castro, J., Albaladejo, G., & Parejo, D. (2020). Precise cache detection by olfaction in a scatter-hoarder bird. *Animal behaviour*, *167*, 185-191. https://doi.org/10.1016/j.anbehav.2020.07.002

Mortensen, A., & Blix, A. J. (1986). Seasonal Changes in Resting Metabolic Rate and Mass-Specific Conductance in Svalbard Ptarmigan, Norwegian Rock Ptarmigan and Norwegian Willow Ptarmigan. *Ornis Scand*, *17*(1), 8-13. https://doi.org/10.2307/3676746

Mortensen, A., Nordoy, E. S., & Blix, A. S. (1985). Seasonal Changes in the Body Composition of the Norwegian Rock Ptarmigan Lagopus mutus. *Ornis Scand*, *16*(1), 25-28. https://doi.org/10.2307/3676571

Mortensen, A., Unander, S., Kolstad, M., & Blix, A. S. (1983). Seasonal Changes in Body Composition and Crop Content of Spitzbergen Ptarmigan Lagopus mutus hyperboreus. *Ornis Scand*, *14*(2), 144-148. https://doi.org/10.2307/3676018

Murrish, D., & Schmidt-Nielsen, K. (1970). Exhaled air temperature and water conservation in lizards. *Respiration Physiology*, *10*, 151-158.

Murrish, D. E. (1973). Respiratory heat and water exchange in penguins. *Respiration Physiology*, *19*(3), 262-270. https://doi.org/10.1016/0034-5687(73)90030-3

Negus, V. E. (1958). *Comparative Anatomy and Physiology of the Nose and Paranasal Sinuses*. E.&S. Livingstone Ltd.

Nord, A., & Folkow, L. P. (2018). Seasonal variation in the thermal responses to changing environmental temperature in the world's northernmost land bird. *J Exp Biol*, *221*(1). https://doi.org/10.1242/jeb.171124

Norderhaug, M. (1984). *Svalbard*. Universitetsforlaget. https://urn.nb.no/URN:NBN:no-nb_digibok_2007041310001

Owerkowicz, T., Musinsky, C., Middleton, K., & Crompton, A. (2014). Respiratory Turbinates in Extant Mammals and Birds. In E. L. Brainerd, K. Dial, & N. H. Shubin (Eds.), *The Great Transformations in Vertebrate Evolution*. University of Chicago Press.

Pedersen, H. C., Follestad, A., Lorentsen, S.-H., Nilsen, E. B., & Stokke, B. G. (2021). *Statusoversikt for jaktbart småvilt: Bestandsstatus og utviklingstrender siste 5 år* (NINA Rapport 1917). Norsk institutt for naturforskning. https://hdl.handle.net/11250/2733527

Peters, J., Lebrasseur, O., Deng, H., & Larson, G. (2016). Holocene cultural history of Red jungle fowl (Gallus gallus) and its domestic descendant in East Asia. *Quaternary science reviews*, *142*, 102-119. https://doi.org/10.1016/j.quascirev.2016.04.004

Prinzinger, R., Preßmar, A., & Schleucher, E. (1991). Body temperature in birds. *Comparative Biochemistry and Physiology Part A: Physiology*, *99*(4), 499-506. https://doi.org/10.1016/0300-9629(91)90122-S

R Core Team. (2020). *R: A language and environment for statistical computing*. In R Foundation for Statistical Computing. https://www.R-project.org/

Rosen, A. D. (1981). Notes on Technic: End-Point Determination in Edta Decalcification Using Ammonium Oxalate. *Stain Technology*, *56*(1), 48-49. https://doi.org/10.3109/10520298109067275

Rossner, M., & Yamada, K. M. (2004). What's in a Picture? The Temptation of Image Manipulation. *J Cell Biol*, *166*(1), 11-15. https://doi.org/10.1083/jcb.200406019

RStudio Team. (2020). *RStudio: Integrated Development Environment for R*. In RStudio, PBC. http://www.rstudio.com/

Saalfeld, S., Burri, O., Eglinger, J., Hiner, M., Preibisch, S., Reuden, C., & Schindelin, J. (2022). *Enhanced Local Contrast (CLAHE)*. Retrieved 28th Apr 2022 from https://imagej.net/plugins/clahe

Schmidt-Nielsen, K., Hainsworth, F., & Murrish, D. (1970). Counter-current heat exchange in the respiratory passages: Effect on water and heat balance. *Respiration Physiology*, *9*, 263-276.

Schneider, C. A., Rasband, W. S., & Eliceiri, K. W. (2012). NIH Image to ImageJ: 25 years of image analysis. *Nat Methods*, *9*(7), 671-675. https://doi.org/10.1038/nmeth.2089

Scholander, P. F., Hock, R., Walters, V., & Irving, L. (1950). Adaptation to cold in arctic and tropical mammals and birds in relation to body temperature, insulation, and basal metabolic rate. *Biol Bull*, *99*(2), 259-271. https://doi.org/10.2307/1538742

Skog, E. B., & Folkow, L. P. (1994). Nasal heat and water exchange is not an effector mechanism for water balance regulation in grey seals. *Acta Physiol Scand*, *151*(2), 233-240. https://doi.org/10.1111/j.1748-1716.1994.tb09742.x

Smith, E. K., O'Neill, J. J., Gerson, A. R., McKechnie, A. E., & Wolf, B. O. (2017). Avian thermoregulation in the heat: resting metabolism, evaporative cooling and heat tolerance in Sonoran Desert songbirds. *J Exp Biol*, *220*(18), 3290-3300. https://doi.org/10.1242/jeb.161141

Solberg, S. B. B., Kjelstrup, S., Magnanelli, E., Kizilova, N., Barroso, I. L. C., Acquarone, M., & Folkow, L. P. (2020). Energy efficiency of respiration in mature and newborn reindeer. *J Comp Physiol B*, *190*(4), 509-520. https://doi.org/10.1007/s00360-020-01284-3

Sulloway, F. J. (1982). Darwin and His Finches: The Evolution of a Legend. *Journal of the History of Biology*, *15*(1), 1-53.

Van Valkenburgh, B., Curtis, A., Samuels, J. X., Bird, D., Fulkerson, B., Meachen-Samuels, J., & Slater, G. J. (2011). Aquatic adaptations in the nose of carnivorans: evidence from the turbinates. *J Anat*, *218*(3), 298-310. https://doi.org/10.1111/j.1469-7580.2010.01329.x

Vömel, H. (2011, 1st Dec). *Saturation water vapor pressure formulations*. University of Colorado. Retrieved 14th Feb 2022 from https://www.eas.ualberta.ca/jdwilson/EAS372_13/Vomel_CIRES_satvpformulae.html

Walker, J. E. C., Wells, R. E., & Merrill, E. W. (1961). Heat and water exchange in the respiratory tract. *The American Journal of Medicine*, *30*(2), 259-267. https://doi.org/10.1016/0002-9343(61)90097-3

Watanabe, T., Takahashi, N., Minaguchi, J., Mochizuki, A., & Hiramatsu, K. (2020). Three-Dimensional Analysis of the Nasolacrimal Duct and Nasal Cavity and Arrangement of Mucosal Tissue in Chickens. *J Poult Sci*, *57*(4), 303-309. https://doi.org/10.2141/jpsa.0190091

Wickham, H. (2016). *ggplot2: Elegant Graphics for Data Analysis*. Springer-Verlag New York.

Young, B., Lowe, J., Stevens, A., & Heath, J. (2006). *Wheater's Functional Histology: A Text and Colour Atlas* (5th ed.). Churchill Livingstone Elsevier.

Appendix

The macro editor for the plugin CLAHE applied to all images in an image sequence imported to ImageJ (Saalfeld et al., 2022):

```
blocksize = 127;
histogram_bins = 256;
maximum_slope = 3;
mask = "*None*";
fast = true;
process_as_composite = true;

getDimensions( width, height, channels, slices, frames );
isComposite = channels > 1;
parameters =
  "blocksize=" + blocksize +
  " histogram=" + histogram_bins +
  " maximum=" + maximum_slope +
  " mask=" + mask;
if ( fast )
  parameters += " fast_(less_accurate)";
if ( isComposite && process_as_composite ) {
  parameters += " process_as_composite";
  channels = 1;
}

for ( f=1; f<=frames; f++ ) {
  Stack.setFrame( f );
  for ( s=1; s<=slices; s++ ) {
    Stack.setSlice( s );
    for ( c=1; c<=channels; c++ ) {
      Stack.setChannel( c );
      run( "Enhance Local Contrast (CLAHE)", parameters );
    }
  }
}
```

Explanation of parameters in the plugin CLAHE

The following explanations are inspired by information from Saalfeld et al. (2022), integrated with personal understanding of how CLAHE works based on experience from using the plugin in ImageJ.

Block size: the histogram for the local region around each pixel is equalized. The size of this region is determined by block size. A small number, like 30, means that the region around each pixel is large, so that the histogram used covers more area. Hence, fewer features in the image are preserved. A larger number then preserves more features.

Histogram bins: this is connected to the total amount of intensity values, which in grey-scale pictures are 256 (0 = black and 255 = white, with a spectrum of different shades of grey between them). Values higher than this are therefore insignificant. It is, as stated by Saalfeld et al. (2022) “the number of histogram bins used for histogram equalization”. Fewer bins, e.g., 50, result in fewer intensity values (only 50 instead of the 256 possible ones), and hence loss of contrast.

Maximum slope: limits what CLAHE can do in terms of contrast changes. A value of 1 gives the original image, and higher numbers results in more contrast. This can for example increase the thickness of the conchae in the image, so too large values should be avoided.